LAMINAR CROSS-BUOYANCY MIXED CONVECTION AROUND A CONFINED TRIANGULAR BLUFF BODY

A DISSERTATION

submitted in partial fulfillment of the
requirement for the award of the degree
of

MASTER OF TECHNOLOGY

in

CHEMICAL ENGINEERING

(With specialization in Computer Aided Process Plant Design)

By

TANVEER RASOOL

DEPARTMENT OF CHEMICAL ENGINEERING
INDIAN INSTITUTE OF TECHNOLOGY ROORKEE
ROORKEE-247 667 (INDIA)

May-2014

Declaration

I hereby declare that the work presented in this dissertation entitled **"Laminar cross-buoyancy mixed convection around a confined triangular bluff body"** submitted towards partial fulfillment for the award of the degree of M-Tech. in Chemical Engineering with specialization in Computer Aided Process Plant Design at the Indian institute of Technology, Roorkee (India) is an authentic record of my original work carried out under the guidance of **Dr. A. K. Dhiman** (IIT Roorkee). I have not submitted the matter embodied in this dissertation for the award of any other degree.

Place: Roorkee (Tanveer Rasool)
Date: 08-05-2014, Enrol. No. 12514026

Certificate

This is to certify that Mr. Tanveer Rasool (Enrol. No. 12514026) has completed the dissertation entitled **"Laminar cross-buoyancy mixed convection around a confined triangular bluff body"** under my supervision.

(**Dr. Amit Kumar Dhiman)**
Associate Professor,
Deptt. of Chemical Engineering
IIT Roorkee

Acknowledgement

It is with great affection and appreciation that I acknowledge my indebtedness and sincere gratitude to my project supervisor Dr. A. K. Dhiman who inspired me to work on the project **"Laminar cross-buoyancy mixed convection around a confined triangular bluff body"**. Even after being quite aware of the topic, the task of the project was mind stimulating and it would not have been possible for me to complete my dissertation work without his encouragement, guidance and support. I wish to express my thanks to Dr. V. K. Agrawal (Professor & Head of the Department) for providing me with an opportunity and the resources for completing this dissertation work.

I would also like to thank my colleagues/scholars, who also work in the same laboratory Malik Parveez, Manu K. Sukesan, Deepak Kumar, Ram Pravesh Ram, Aniruddha Sanyal and Vivek Verma for their valuable suggestions and help as and when required.

I would like to take this opportunity to recognize the selfless support of my family members especially my parents and my elder brother Dr. Akhtar Rasool. The work would not have been possible without their love and prayers. I convey special acknowledgment to my in-laws especially my mother in law, who supported my family by their unconditional love and support when I was away. My wife Syed Rifat and my son Master Farhaan deserve special mention for their support, patience, love and prayers.

Finally I owe my sincere thanks to my parent institute National Institute of Technology, Srinagar (J&K) for sponsoring my higher studies.

Tanveer Rasool
En. No. 12514026
M.Tech (C.A.P.P.D)

CONTENTS

List of Figures

List of Tables

Abstract

The numerical simulations in 2-D are carried out to investigate the effects of cross-buoyancy on the flow and heat transfer characteristics over an equilateral triangular bluff body placed at the central axis of horizontal channel with its vertex facing the flow, at low and intermediate Reynolds numbers. The results are generated for the ranges of control parameters as $1 \leq Re \leq 150$ and Richardson number (Ri) = 0-2. The pressure-velocity coupling equations are resolved by using SIMPLE algorithm on a collocated grid system. The variations in overall drag coefficients, lift coefficients, Strouhal number and average Nusselt number are found and discussed for the preceding conditions, to conclude as to how the control parameters like Reynolds and Richardson numbers effect the confined flow and heat transfer phenomena. For all the three Richardson numbers studied, it was found that there is a decrease in overall drag coefficient with increasing Reynolds number up to around Re=100. Thereafter the total drag coefficient (C_D) shows an increasing trend. For a fixed Richardson number (Ri), an average Nusselt number ($\overline{Nu}$) is found to increase with increasing Reynolds number. However, at any fixed Reynolds number an average Nusselt number shows soft but varying response towards increasing buoyancy (Ri>0). The percentage enhancement of approximately 3% in an average Nusselt number is found for Re=40, for all values covered under this study while comparing the values of average Nusselt number at Ri=1 and 2 with respect to that at Ri=0. A simple heat transfer correlation is given to relate the values of $\overline{Nu}$ and Re for Richardson numbers 1 and 2. Furthermore, extensive simulations have been carried out to calculate the critical Reynolds numbers (Re_c) showing the transition of flow from a symmetric to a periodic regime with changing Richardson numbers. As the critical Reynolds number for the forced convection (Ri=0) is reported elsewhere (Srikanth et al. 2010), for the mixed convection the Re_c values lie between Re=61 and 62 for Ri=1 and between Re=90 and 91 for Ri=2.

Key words: Triangular bluff body; Cross-buoyancy; Confined flow; Critical Reynolds number; Drag and lift coefficients and Heat transfer enhancement.

Nomenclature

b	a side of an equilateral triangular cylinder, m
C_p	specific heat of the working fluid, J kg^{-1} K^{-1}
C_D	drag coefficient ($=2F_D /\rho U^2_{max} b$)
C_{DF}	frictional drag coefficient
C_{DP}	pressure drag coefficient
C_L	lift coefficient ($=2F_L/ \rho U^2_{max} b$)
f	vortex shedding frequency, s^{-1}
F_D	drag force per unit length of triangular cylinder, Nm^{-1}
F_L	lift force per unit length of the cylinder, Nm^{-1}
g	acceleration due to gravity, ms^{-2}
Gr	Grashof number ($=\rho^2 g\beta(T_w - T_\infty)b^3/\mu^2$)
h	local heat transfer coefficient, Wm^{-2} K^{-1}
$\bar{h}$	average heat transfer coefficient, Wm^{-2} K^{-1}
H	height of the domain used, m
k	thermal conductivity of the working fluid, $Wm^{-1}K^{-1}$
L	length of the domain used, m
Nu	local Nusselt number ($=hb/k$)
$\overline{Nu}$	average Nusselt number ($=\bar{h}b/k$)
p	pressure ($=p^*/(\rho U^2_{max})$)
Pr	Prandtl number ($=\mu C_p/ k$)
Re	Reynolds number ($=\rho U_{max} b/\mu$)
Re_c	Critical Reynolds number

Ri	Richardson number (= Gr/Re^2)
St	Strouhal number (=fb/U_{max})
T^*	Temperature, K
T_∞	temperature of the working fluid at inlet, K
T^*_w	constant wall temperature at the surface of the triangular cylinder, K
t	time (=$t^*/(b/U_{max})$)
T_p	time period for one cycle
U_{max}	maximum velocity of the fluid at the channel inlet, ms^{-1}
V_x	component of velocity in the direction of x-axis (=V^*_x /U_{max})
V_y	component of velocity in the direction of y-axis (=V^*_y /U_{max})
x	stream-wise coordinate (=x^*/b)
X_d	downstream distance of the triangular cylinder, m
X_u	upstream distance of the triangular cylinder, m
y	transverse coordinate (=y^*/b)

Greek symbols

θ	temperature {=$(T^* - T_\infty)/(T^*_w - T_\infty)$}
β	blockage ratio (=b/H)
ρ	density of the fluid, kgm^{-3}
μ	viscosity of the fluid, $kgm^{-1}s^{-1}$

Superscript

*	dimensional variable

Publications

International journals:

1. T. Rasool, A. K. Dhiman and M. Parveez, Cross-buoyancy mixed convection around a confined triangular bluff body, Numerical Heat Transfer Part-A (Under review).

Conference:

1. T. Rasool, A. K. Dhiman and M. Parveez, Simulation of forced convection heat transfer from a confined triangular bluff body in a channel, Proceedings of the National conference on Innovations and Development in Chemical Technology, PP 114-118, Feb. 28-March 01, 2014, GGIPU, Dwarka Delhi.

CHAPTER 1

INTRODUCTION

The study of combined free and forced (or mixed) convection around different geometrical bluff bodies in an enclosure has been a topic of considerable attention of researchers in recent times due to its fundamental and pragmatic relevance. It is one of most important subjects that has been studied both numerically and experimentally. The bluff bodies when placed in different fluid streams, generate different kind of fluid flow separation over a substantial portion of their surfaces, depending on their shapes. For example, the separation of the fluid flow occurs from fixed points in an edged cylinders (triangular and trapezoidal cross-section etc.) whereas for cylinders having continuous surface curvature (circular or elliptical cross-section etc.), the flow separation depends on the shape of the bluff body and the state of boundary layer generated. The application of these studies has proven to be of great importance in understanding the effects of various parameters on the performance of thermal equipment in various engineering applications. These include heat exchangers, solar heating systems, boilers based on natural circulation, dry cooling towers, nuclear reactors , off-shore structures and flow metering devices etc. Similar other related problems and their studies have found applications in crop dryers, energy storage devices, crude oil storage tanks and flow dividers. The studies of researchers reveal that there exist lot of parameters which directly affect the heat transfer and flow patterns of the systems including obstacles or bluff bodies. Some of the important parameters include the nature of fluid (Newtonian or non-Newtonian), the shape of the bluff body, Reynolds number of the fluid, the blockage ratio, aspect ratio of the bluff body etc. The vast literature is available highlighting the study of forced and/or mixed convection across different shaped bluff bodies in enclosures with either cross buoyancy or aiding buoyancy flow and heat transfer with either vertical or the horizontal imposed heat flux/temperature difference. The present study has been taken up to find a correlation to report the mixed convection heat transfer and fluid flow under laminar cross-buoyancy over a heated equilateral triangular cylinder (aspect ratio=1) in a channel (horizontal) for laminar range of Reynolds numbers and other parameters for which no data is available. This study has been carried out for a fluid with constant Prandtl number of 0.71(air). The objective is to investigate numerically the effects of wall confinements on the flow and mixed convection from an equilateral triangular bluff body for laminar flow regime. The study also includes the

presentation of flow separation at different values of Reynolds number and Richardson number at fixed blockage ratio of 25%. Extensive simulations have been carried out to report the variation of some important parameters like overall drag coefficients, lift coefficient, Strouhal number and average Nusselt number etc. with increasing buoyancy (Richardson number). The ultimate goal of this project is to provide a good description of the influence of Reynolds numbers and Richardson numbers on the fluid-structure interaction and the heat transfer between the two.

A brief description of the related terms used in the subsequent chapters is presented herein.

1.1 Newtonian fluid

Newtonian fluids are those fluids which obey the Newton's law of viscosity which states that the shear stress acting on the surface of flowing fluids is directly proportional to the negative of velocity gradient and obeys the following equation

$$\tau = \mu\left(\frac{dv}{dy}\right)$$

The equation is called Newton's equation of viscosity, where τ is shear stress, μ is the viscosity of fluid and $\left(\frac{dv}{dy}\right)$ is the shear rate or velocity gradient.

All gases and most liquids that have simple molecular formula and low molecular weight are Newtonian fluids. Examples of Newtonian fluids are water, benzene, hexane, ethyl alcohol, carbon tetra chloride etc. Certain fluids among them which are of great practical importance, such as water and air, have very small coefficients of viscosity. In many instances, the motion of such fluids of small viscosity agrees very well with that of an ideal or perfect fluid. For this reason the existence of viscosity is completely neglected in the theory of perfect fluids, mainly because this introduces a far-reaching simplification of the equations of motion, as a result of which an extensive mathematical theory becomes possible. Most theoretical investigations in the field of fluid mechanics are based on the concept of a perfect, i.e. frictionless plus incompressible, fluid. In the motion of such a perfect fluid, two contacting layers experience no or minimal tangential forces (shearing stress) but act on each other with normal forces (pressures) only.

1.2 Drag coefficient and bluff body flow

In various engineering applications, situations are encountered where in Newtonian/non-Newtonian fluids flow around submerged bodies/objects. In such cases either the fluid flows around a stationary body or the obstacle moves through a bulk of fluid at rest. Sometimes both the fluid as well as the body may also be in motion. Relative motion between a real fluid and a body brings into action a thrust exerted by the flowing fluid on the bluff body. Simultaneously, a body exerts an equal and opposite force on the fluid. Hence, a submerged body may be subjected to drag and lift forces. A body placed in any fluid is subjected to a drag force, which usually comprises of two parts: frictional drag and pressure drag. The frictional drag force is due to the friction between the fluid flowing and the surfaces over which it flows. The friction is generated due to the development of boundary layers, which scales with increasing Reynolds number. Pressure drag is an outcome of eddy motions that are generated in the fluid as it passes the bluff body. This pressure drag is usually less sensitive to any change in the Reynolds number than its other part, the frictional drag. Formally, both the types of drag are because of the viscosity of the fluid, however distinction is necessary as both the parts of the overall drag are due to different phenomena of fluid flow. Frictional drag is important for attached flows with no separation of flow and is influenced by the surface area exposed to the flow. On the other hand, the pressure drag is important for separated flows and is influenced by the shape and cross-sectional area of the bluff body.

When the overall drag coefficient is dominant by viscous drag, the body is said to be *streamlined*, and when the drag is dominant by pressure drag, the body is said to be *bluff*. Therefore the nature of the flow i.e. whether it is viscous-drag dominant or pressure-drag dominant depends purely on the shape of the bluff body and for a given frontal area and velocity, a body with a streamlined shape, always shows lesser resistance than a bluff body. Spheres and cylinders are considered bluff bodies while as fish like bodies and air foils at small angles of attack are considered as streamline bodies. In the present study, the bluff body is an equilateral triangular cylinder with some streamline features.

An another aspect of a bluff body is that a boundary layer separation is always experienced when a fluid flows past it. When a boundary layer extends far enough against an adverse pressure gradient in such a manner that the growth of the boundary layer relative to an object falls almost to zero, flow separation is said to occur [1, 2]. The flow detaches from the surfaces of a bluff

body and giving rise to eddies and vortices. This flow separation often results in increased drag coefficient, particularly the pressure drag which is due to the difference in pressure between the front and the rear surfaces of the bluff body as it moves through the fluid. In order to reduce the effect of the flow separation and keep local flow attached to the body as long as possible, much effort and research has already been carried out for designing of such aerodynamic surfaces which are responsible for delaying of the flow separation. Some examples include the dimpled golf ball, fur on tennis balls, tabulators on glider which induce an early transition to turbulent flow regime and similarly vortex generators fitted on small aircrafts to control the separation of flow etc.

1.3 Wake

A wake is the area of turbulence formed at the rear end of any bluff body placed in the moving fluid. The wake is a disturbed fluid usually formed in the downstream region of the confined flows across the moving or stationary bluff bodies. The formation of these wakes in incompressible fluids is analogous to the generation of shockwaves in compressible fluids or flow, such as the shockwaves generated by aircraft and rockets traveling through air. The wake is also termed as recirculation length and is the measure of the length between the rear surface of the bluff body to the point of attachment for the closed streamline on the axis of the symmetry. The location of the attachment point is determined computationally by monitoring the stream wise velocity along the stream wise centerline of the bluff body and moving downstream until the sign changes from negative to positive.

1.4 Dimensionless Groups

The dimensional considerations of the flow and simple scaling is done to characterize the flow by introducing various dimensionless numbers. The dimensionless numbers used in the present study are briefly described as follows.

1.4.1 Reynolds Number (Re)

The Reynolds number may be defined for several different situations where a fluid moves relatively with respect to any surface and the definitions generally include the fluid properties

like velocity, density, viscosity, etc. and a characteristic length of the body. For flow in a tube or a channel, the Reynolds number is given generally as:

$$Re = \frac{\rho U b}{\mu}$$

The transitional parameter related to Reynolds number is termed as critical Reynolds number and is denoted as Re_c. Thus the critical Reynolds number is that value of Re wherein flow changes its behaviour from steady to unsteady (periodic) type. In the present study the Reynolds number is limited to 150. However an extensive simulations are carried out to calculate the critical Reynolds numbers when buoyancy is introduced in the system.

1.4.2 Prandtl number (Pr)

The Prandtl number is simply the ratio of momentum diffusivity (kinematic viscosity) to thermal diffusivity and is given as:

$$Pr = \frac{\mu C_p}{k}$$

The fixation of the value of Prandtl number in simulation studies generally defines the working fluid being used. The typical values of Prandtl number for various fluids varies between 0.015 for Mercury to 40000 for engine oils. The present study has been carried out with air as a fluid with a constant Prandtl number of 0.71. Moreover in heat related problems, the Prandtl number is said to controls the relative thickness of the thermal and momentum boundary layers.

1.4.2 Strouhal number (St)

The values of Strouhal number are useful for analyzing oscillations generated in unsteady fluid flow problems. The Strouhal number is defined as the ratio of inertial forces generated because of the unsteadiness of the fluid flow to that of inertial forces which are due to the changes in velocity from one point to an another in the flow field. The periodicity in the flow field is induced as a result of the vortex-shedding phenomena and is given in the form of Strouhal number (St) as:

$$St = \frac{fb}{U}$$

1.4.3 Nusselt number (Nu)

Nusselt number is dimensionless parameter used in calculating the heat transfer between a moving fluid and a solid body and is represented as:

$$Nu = \frac{hb}{k}$$

Within a fluid, Nusselt number at a boundary is given as the ratio of convective to conductive heat transfer across that boundary. A larger Nusselt number corresponds to more active convection while as the values of Nusselt number close to unity, corresponds to almost equal magnitudes of convection and conduction and is the property of slug or laminar flow. Nusselt number is the most commonly used dimensionless number to represent the heat transfer data for a definite set of conditions in terms of correlations. There are many, many correlation equations. Each is for a specific application and is valid under specified conditions. In the present study a simple correlation in terms of Nusselt number is presented to evaluate heat transfer for the range of conditions used.

An average Nusselt number represented by $\overline{Nu}$ for a steady flow in the present study represents the average of local Nusselt number over surfaces of whole triangular cylinder and finally the average cylinder Nusselt number is calculated by averaging these values.

1.4.4 Richardson number (Ri)

In thermal convection problems, the Richardson number (Ri) elucidates the importance of the natural convection to that of forced convection. It is the dimensionless number, expressed as the ratio of potential energy to kinetic energy and is given as

$$Ri = \frac{Gr}{Re^2} = \frac{g\beta\Delta Tb}{U^2}$$

The Richardson number signifies the role of buoyancy in the flow. If the value of Richardson is zero, the buoyancy is does not affect the flow and the heat transfer is termed as forced convection. As the value of Richardson number increases (Ri>0), buoyancy is dominant and aids in flow mixed convection. An infinite value of Richardson number represents free convection. The present study has been carried out to focus on the effects of cross-buoyancy mixed convection (Ri) on the fluid flow and heat transfer and the range studied is Ri=0, 1 and 2.

CHAPTER 2

LITERATURE REVIEW

The two-dimensional (2-D) forced and mixed convection heat transfer in laminar regime around an triangular cylinder of equal edges in a horizontal channel with air as working fluid is a very basic configuration studied by many researchers in detail.

Abbassi et al. [3] studied forced convection (Ri=0) flow and heat transfer for two Reynolds numbers, Re=30 and Re=100 as the samples of the symmetric and periodic asymmetric flow respectively for a triangular cylinder with an aspect ratio of 0.5. The results report that the presence of a triangular cylindrical effects both the symmetric as well as asymmetric or periodic flow and heat transfer as the heat flows from hot bottom plate to the fluid. Subsequently, Abbassi et al. [4] carried out another study of the same system for finding out the influence of Grashof numbers (Gr) on the fluid flow and heat transfer in a plane channel with a built-in triangular cylinder. An important aspect of their work is that the triangular bluff body, the top wall along with the incoming fluid stream are assumed to be at a constant temperature, whereas the bottom wall is assumed hot and at a higher temperature. For this configuration, their study at Re=100, $0 \leq Gr \leq 1.5x10^4$ and Pr=0.71 reveals that the effects of thermal buoyancy slightly increases the frequency of vortex shedding and the presence of a triangular prism is responsible for about 44% increase of the time-averaged Nusselt number. De and Dalal [5] made a numerical investigation of forced convection fluid flow and heat transfer in laminar regime from an equilateral triangular bluff body placed in a horizontal channel for the range $80 \leq Re \leq 200$, but for different blockage ratios of 8.33% - 33.33%. The fluid used for working out the solutions was air having a fixed Prandtl number of 0.71. The Strouhal number (St) and root mean square (rms) lift coefficient is reported to increase significantly with blockage ratio and Reynolds number, while the blockage ratio has negligible effects on the time-averaged Nusselt number. Their study shows that the St-Re relationship has a flat maximum around Re=130 for $\beta<16.66\%$, whereas it increases monotonically for $\beta \geq 16.66\%$ with Re. A numerical investigation by Farhadi et al. [6] found the removal of vortex shedding along with the subsequent decrease in the rate of heat transfer occurring at lower Reynolds number by approaching triangular cylinder in the wall. The computations were carried out for Reynolds number range of 100-450 at various gap widths of

0.5, 0.75 and 1. The results also reveal that the variations in vortex formation effects the skin friction coefficient to a larger extent than the Nusselt number. At low Re (1-80), Srikanth et al. [7] simulated the fluid flow and heat transfer forced convection phenomena (Ri=0) of air (Pr=0.71) across an equilateral triangular cylinder placed in a horizontal channel . The blockage ratio of the triangular cylinder was fixed as 25%. The critical Reynolds number (Re_c) was found lying between Re=58 and 59 for above set of conditions. The wake length and an average Nusselt number was reported to increase with Reynolds number for the set of conditions considered. Chattopadhyay [8] numerically investigated the presence of a triangular prism in a channel, but in a turbulent regime for Re up to 40000 with an air as working fluid having Pr=0.71. The study has been carried on an isosceles triangle with an aspect ratio of 4.0. The results reveal that because of the triangular cylinder, rate of heat transfer in a channel is augmented by around 15% and is also responsible for vortex formation downstream of the triangular prism. Ali et al. [9] investigated numerically the 2-D unconfined forced convection heat transfer around a horizontal equilateral triangular bluff body placed in air (Pr=0.71) under laminar conditions of the flow ($Re \leq 200$). the study was done for two configurations of the cylinder: one with the vertex facing the fluid flow and the other when flat base of the cylinder faces the fluid flow. The former configuration which is of our interest has been evaluated and heat transfer data is generated and presented in the form of average Nusselt number versus Reynolds numbers. They reported that with an increase in Reynolds number, streamlines lose their symmetry about the centre line because of the role of convective terms becoming distinct. The overall drag coefficient is reported to decrease with increasing Reynolds number till certain symmetrical limiting values and thereafter shows an increasing trend. Lastly, Nusselt number correlation is provided. The unsteady 2-D numerical simulations were performed by Chatterjee and Mondal [10] to investigate the heat transfer at Ri=0 (forced convection) past a long heated equilateral triangular cylinder but in an unconfined medium for low Reynolds numbers. The Reynolds number range considered for the study was from 50 to 250 but for three varying values of Prandtl numbers (Pr = 0.71,7 and 100). The main findings to mention here include the increase in local Nusselt number and the amplitude of oscillations of both drag and the lift coefficients while increasing the Reynolds number. The Strouhal number was reported to increase at a quicker rate initially up to Re=100, then at a slower rate until it reaches a maximum value of about Re=150 and thereafter it reportedly falls down. Recently, the effects of blockage

ratios (β=12.5%-50%) on the fluid flow of non-Newtonian / power-law fluids over an equilateral triangular cylinder conned in plane channel were investigated by Dhiman and Kumar [11]. They reported the results for Re ranging from 1 to 40 in the 2-D laminar regime. Extensive numerical results highlight the changes in flow patterns, wake length, individual and overall drag coefficients and the variation of pressure coefficients on the surface of a long triangular cylinder to make clear the combined effects of Reynolds number and blockage ratio.

Experimentally, El-Sherbiny [12] investigated the average pressure distribution on the edges of a 90^0 triangular prism in a uniform smooth fluid flow at higher Reynolds number of the order of 10^5 with varying the angle of flow incidence from 0^0 to 180^0. The findings revealed that the flow remains fully attached to the two surfaces only when the line bisecting the angle between these surfaces is parallel to the incident fluid flow. However, for all other cases the flow separates from the corner of the triangular cylinder giving rise to the formation of bubble. The flow reattaches to the side downstream of that corner, characterized by local inflation in both average and fluctuating pressures. Csiba and Martinuzzi [13] obtained phase averaged velocity and surface pressure data for higher Reynolds number of 22500. The angle of incidence of fluid on the triangular cylinder was adjusted to fix the relative intensity of the shear layers. It was also reported that by using the projected obstacle width, the vortex shedding frequency can satisfactorily be scaled. In another experimental study at a Reynolds number of approximately $1.2x10^5$, wake flow features of low aspect ratio triangular prism were investigated by Lungo and Buresti [14]. They reported that the vortex shedding frequency is a function of the low orientation in strict relation with the changes of the width of the wake and that it shows an increasing trend with decreasing aspect ratio. Hassab et al. **[**15] carried out an experimental investigation of mixed convection heat transfer from an isothermal triangular cylinder kept in a horizontal channel. The study has been carried out for three equilateral triangular cylinders with side length of 37, 50 and 70 mm with Grashof numbers ranging from $26.32x10^4$ to $213.46x10^4$,Reynolds number range was fixed from 75.3 to 1251.6 and attack angles from 0^0 to 180^0. The experimental results showed the average Nusselt number for air (Pr= 0.7) as a working fluid. The results show that the heat transfer by conduction is unchanged with Reynolds number but the heat transfer by convection increases with the angle of attack. Convective heat transfer also gets affected by Reynolds number and Grashof number. For same Reynolds number , as the attack angle of the air flow increases the Nusselt number decreases. At low Reynolds number , the

natural convection is dominant .They further concluded that by increasing the side length of the triangle, the average Nusselt number increases at the same Reynolds and Richardson number.

The effects of cross-buoyancy on forced and mixed convection around the geometries other than triangular cylinders have been investigated and reported thoroughly in the literature. For instance, Dhiman et al. [16] investigated the effects of cross-buoyancy and Prandtl number on the fluid flow and the mixed convection heat transfer around a confined isothermal square cylinder. The results are presented for $1 \leq Re \leq 30$, $0.7 \leq Pr \leq 100$ and $0 \leq Ri \leq 1$. The fixed blockage ratio of 12.5% was used. The study apart from highlighting the role of the mentioned dimensionless numbers on the fluid flow and heat transfer, found that the drag coefficient is less responsive to Richardson number than the lift coefficient for the similar set of parameters. In an another study, Chatterjee and Mondal [17] followed the role of thermal buoyancy on the vortex shedding across a square cylinder in a cross flow for the following ranges control parameters: $5 \leq Re \leq 40$, $0 \leq Ri \leq 2$ and for constant Prandtl number of 0.7 (air). The fluid flow and heat transfer characteristics are reported to change appreciably with the introduction of thermal buoyancy. The critical Richardson number responsible for the onset of vortex shedding is found to decrease with increasing Reynolds number. Similarly computer simulations of expanded trapezoidal body under cross-buoyancy by Dhiman and Ghosh [18] was carried out recently to investigate the effects of cross-buoyancy on various parameters.

In all the papers cited above, there seems very limited work available to report the mixed convection flow and heat transfer under the influence of cross-buoyancy over a heated equilateral triangle in a horizontal channel (confined flow) for low or intermediate Reynolds numbers with varying Richardson numbers, which motivates the current study. In particular, only Abbassi et al. [4] and Srikanth et al. [7] investigated the transition of flow to periodic unsteady state and are limited to only forced convection (Ri=0) across a confined triangular bluff body. Thus, the first objective of the present study is to investigate the effect of wall confinement on the cross-buoyancy mixed convection from an equilateral triangular obstacle in the steady flow regime. Secondly, how the flow separation sets and varies at different values of Reynolds number, Richardson number and blockage ratio, has been studied. An attempt is finally made to obtain the critical Reynolds numbers (Re_c) for the onset of periodic unsteady flow over a triangular shaped obstacle with changing Richardson number, which is yet to be reported in the literature. Moreover, the variation of some important output parameters like total drag and lift

coefficients, average Nusselt number and representative streamlines and isothermal contours are presented to observe the effects of varying Richardson numbers around a confined equilateral triangular bluff body in the cross-buoyancy. The frequency of vortex shedding (Strouhal number) is also reported and discussed. The study of flow and thermal patterns by way of streamlines and isothermal contours is an important part of this dissertation work. In the end, a heat transfer correlation has been presented relating the preceding range of conditions.

CHAPTER 3

PROBLEM STATEMENT AND NUMERICAL MATHODS

3.1 Problem statement and mathematical formulation

The schematic diagram for the flow around an equilateral triangular bluff body in a horizontal channel is shown in Fig.1. Since the obstacle is of equilateral cross-section, an aspect ratio is equal to 1. The blockage ratio (β=b/H) is fixed as 25%. The vertex of an equilateral triangular cylinder with side b (the non-dimensionalizing length scale) is facing the flow. At the inlet, the flow is fully developed and isothermal with a velocity U_{max} and the temperature T_∞, which are also the non-dimensionalizing velocity and temperature scales, respectively. The triangular bluff body is maintained at a constant temperature of T_w ($T_w > T_\infty$). The dimensionless upstream and downstream distances are denoted as X_u/b and X_d/b respectively, whereas the total length of computational domain is L/b in the x-direction. The dimensionless height of the computational domain is given by H/b in the y-direction.

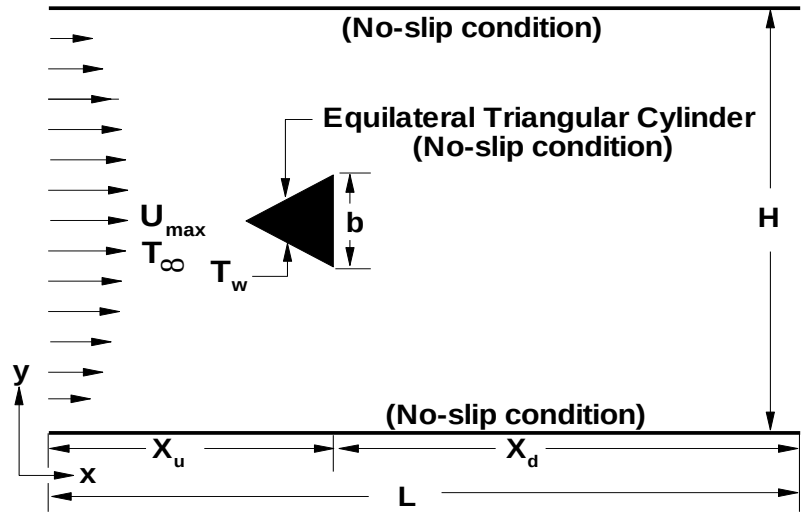

Figure 1: *Schematics of the flow around an equilateral triangular bluff body in the confined domain*

The dimensionless governing continuity, x- component and y- component of Navier-Stokes, and thermal energy equations are given below by equations (1) to (4) for the present system as stated by Bird et al. [19].

Continuity equation :

$$\frac{\partial V_x}{\partial x} + \frac{\partial V_y}{\partial y} = 0 \tag{1}$$

x-Momentum equation :

$$\frac{\partial V_x}{\partial t} + \frac{\partial (V_x V_x)}{\partial x} + \frac{\partial (V_y V_x)}{\partial y} = -\frac{\partial p}{\partial x} + \frac{1}{Re}\left(\frac{\partial^2 V_x}{\partial x^2} + \frac{\partial V^2 V_x}{\partial y^2} \right) \tag{2}$$

y-Momentum equation:

$$\frac{\partial V_y}{\partial t} + \frac{\partial (V_x V_y)}{\partial x} + \frac{\partial (V_y V_y)}{\partial y} = -\frac{\partial p}{\partial y} + \frac{1}{Re}\left(\frac{\partial^2 V_y}{\partial x^2} + \frac{\partial^2 V_y}{\partial y^2} \right) + Ri\theta \tag{3}$$

Energy equation :

$$\frac{\partial \theta}{\partial t} + \frac{\partial (V_x \theta)}{\partial x} + \frac{\partial (V_y \theta)}{\partial y} = \frac{1}{Re\,Pr}\left(\frac{\partial^2 \theta}{\partial x^2} + \frac{\partial^2 \theta}{\partial y^2} \right) \tag{4}$$

The boundary conditions in their dimensionless form may be written as :

a) At the channel inlet : $V_x = 1 - \left(|1 - 2\beta y|\right)^2$ $(0 \le y \le H/b$ and $\beta = b/H)$; $V_y = 0$ and $\theta = 0$

b) On the surface of the triangular cylinder : $V_x = 0,\ V_y = 0$ and $\theta = 1$

c) On the upper and lower boundaries : $V_x = 0,\ V_y = 0$ and $\frac{\partial \theta}{\partial y} = 0$

d) At the exit boundary : $\frac{\partial V_x}{\partial x} = 0, \frac{\partial V_y}{\partial x} = 0$ and $\frac{\partial \theta}{\partial x} = 0$

The heat dissipation is assumed to be negligible and the thermo-physical properties except for the body force term in the momentum equation are assumed to be constant.

3.2 Grid structure and Numerical methodology

A geometry and mesh used for the simulation study is presented in Fig. 2. Geometries were constructed with an aid of Geometry and Model building intelligent toolbox of Ansys Fluent workbench. The grid structure used in this study is an identical one as used in ref. [7]. The mesh is finer towards the body of the triangular cylinder (the region of larger gradient) and coarser towards the domain edges (the region of lower gradient). The computational grid contains total number of 94,794 cells and each edge of the equilateral triangular cylinder contains 100 grid points. A very fine grid size of 0.002b is applied near the top and bottom walls of the channel as well as near the cylinder [7].

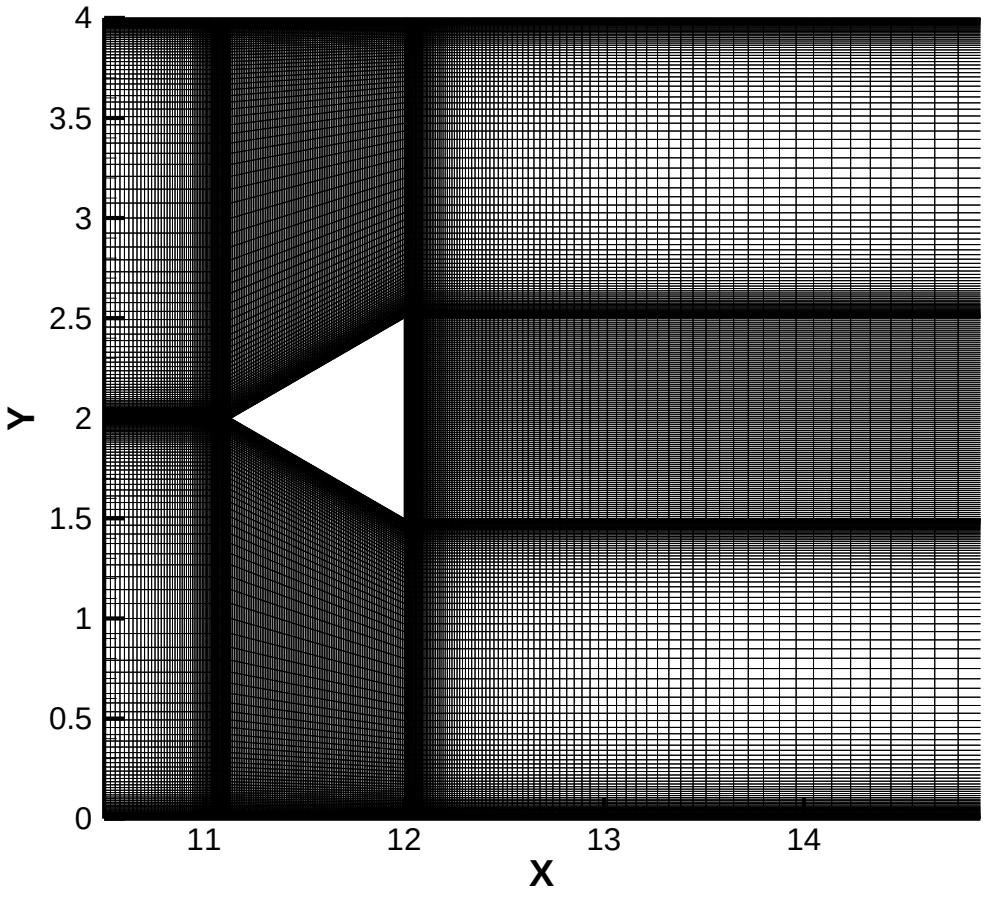

Figure 2: *Grid structure of the problem with blockage ratio of 25%.*

The mass, momentum and energy balance equations are solved using a finite volume solver ANSYS Fluent [20]. The pressure-velocity coupling of equations was resolved by applying SIMPLE (Semi-implicit method for the pressure linked equations) algorithm. The second order implicit time-integration method is applied with the time step of 0.01 (dimensionless) to minimize the effects in the values of the physical output parameters considered [7, 11]. The convective terms are discretized using second order upwind scheme while as the resulting algebraic equations are solved by Guass-Siedel iterative method combined with an Algebraic Multi-Grid solver (AMG). The AMG method is responsible for reducing the time required for obtaining convergence by greatly reducing the number of iterations. The relative convergence criteria of 10^{-20} and 10^{-15} is used for solving the continuity and the x-and y-components of the velocity and the energy equation in the steady regime respectively. While as, the convergence criteria in the case of unsteady flow regime has been taken of the order of 10^{-20} [7, 11].

3.3 Grid and Domain Optimization

The Grid independence study was carried out for two grids of the size of 74,660 cells and 94,794 cells respectively. The smallest grid sizes of 0.004b was investigated near the triangular cylinder while as the grid size of 0.002b was taken towards the top and bottom walls of the channel. The number of grid points on each side of an equilateral triangular cylinder was taken as 100. The results were generated at Re=100 and Re=150 for both the cases which reveal that the percentage relative changes in the values of the mean drag coefficient and the average Nusselt number for the above two cases are negligible. Therefore the grid size of 94,794 cells was applied for the present study.

Table 1: *Effect of downstream distance on the dimensionless output parameters C_D, St, $\overline{Nu}$ for various values of Ri at Re=150.*

Ri	**Output Parameters**	**X_d =20b**	**X_d =25b**	**X_d =30b**
Ri=0	C_D	2.0013	2.0012	2.0013
	St	0.2252	0.2247	0.2247
	$\overline{Nu}$	7.1614	7.1613	7.1614
Ri=2	C_D	1.8598	1.8598	1.8598
	St	0.2293	0.2299	0.2299
	$\overline{Nu}$	7.1612	7.1612	7.1612

The downstream dependence is checked at three values of downstream distances of 20b, 25b and 30b. The study is carried out for Ri=0 and Ri=2 for fixed Reynolds number of 150. Based on the results shown in the Table 1, the optimized downstream domain distance is fixed as X_d=25b. The relative difference in the values of overall drag coefficient and average Nusselt number are found to be less than 0.5% or almost negligible when comparing X_d=20b with X_d=25b and comparing X_d=25 with X_d=30b respectively for fixed Richardson number zero(Ri=0). Similarly the relative difference in the value of overall drag coefficient was found to be less than 0.5% or negligible

for X_d=20b with X_d=25b and X_d=25b with X_d=30b at Richardson number 2(Ri=2).Thus the downstream distance of 25b is found to be adequate for the generation of the results. The Reynolds number has been fixed at 150 in both the cases.

The upstream dependence is checked at two values of upstream distances of 12b and 17b respectively. The study is carried out for Ri=0 and Ri=2 for fixed Re=150.Based on the results as in Table 2, the optimized upstream distance is fixed at X_u=12b.

Table 2: *Effect of upstream distance on the dimensionless output parameters C_D and $\overline{Nu}$ for various values of Ri at Re=1.*

Ri	**Output Parameters**	**X_u=12b**	**X_u=17b**
Ri=0	**C_D**	37.2553	37.2553
	$\overline{Nu}$	0.5392	0.5373
Ri=2	**C_D**	37.2268	37.2270
	$\overline{Nu}$	0.5390	0.5371

The results show that the relative difference in the values of overall drag and average Nusselt number at X_u=12b and X_u=17b is less than 0.5% (Negligible). Therefore an upstream distance of 12b is fixed for the domain under consideration for this study.

Based on the results shown, the optimized values of X_u/b and X_d/b used are 12b and 25b respectively. The overall length of computational domain thus comes out to be 37b in an axial direction.

CHAPTER 4

RESULTS AND DISCUSSION

This study was aimed to conduct a full-domain numerical simulation for studying flow separation and confined mixed convection around an equilateral triangular bluff body under cross-buoyancy for Reynolds number ranging from 1-150 at different Richardson numbers (Ri=0,1 and 2) for a fixed blockage ratio of 25%. As the buoyancy effects decrease with increasing Prandtl number [16, 21, 22], the value of Prandtl number is kept fixed at 0.71 for air, the working fluid for this study. As reported numerically/experimentally [23, 24] that the flow becomes three-dimensional for Reynolds number of around 160 for a sharp edged bluff body of square cross-section, therefore the current study is limited to Re=150.

The calculations for various engineering parameters such as drag and lift coefficients, average Nusselt number and Strouhal number are carried out and discussed for the above range of Reynolds and Richardson numbers. A few representative streamline and isotherm contours are given and described to elucidate the steady and time-periodic fluid flow and thermal variations around an equilateral triangular bluff body for the above mentioned variable parameters. Additional simulations were carried out to report the transitional flow parameters (e.g., critical Reynolds number) for various flows with changing Richardson numbers. Finally, an empirical equation is established which correlates the average Nusselt number with Reynolds and Richardson numbers for the ranges covered under this study.

4.1 Validation

The results generated after numerical simulations are compared with the results reported by De and Dalal [5] and Srikanth et al. [7] for Reynolds numbers 100 and 150. The benchmarking of the present numerical solution procedure is conducted at fixed Richardson number and Prandtl numbers of 0 and 0.71 respectively and the results are presented in Table 3 and 4. The present results when compared with the available literature, shows an acceptable percentage deviation and hence stand validated. For instance, while comparing the values of mean drag coefficients of the present study with literature values shows the relative differences of less than 1.8% for Re=100 and less than 3.4% for Re=150.

Table 3: *Validation of present results of (C_D) and (St) with literature values for unsteady confined flow regimes at Re=100 and 150.*

Re	Source	C_D	% deviation of C_D	St	% deviation of St
100	Present work	1.700	-	0.2036	-
	De and Dalal [5]	1.680	1.17	0.2050	0.68
	Srikanth et al.[7]	1.670	1.72	0.2004	1.57
150	Present work	2.000	-	0.2247	-
	De and Dalal [5]	1.960	2.00	0.2250	0.13
	Srikanth et al.[7]	1.934	3.30	0.2212	1.56

The maximum deviations in the Strouhal number are found to be less than 1.6% for both Re=100 and Re=150. However, deviations in the Nusselt number are less than 0.5% for both Reynold numbers, when comparing with the results given by ref. [7] as shown the Table 4 below.

Table 4: *Validation of present results of ($\overline{\mathrm{Nu}}$) with literature values for unsteady confined flow regimes at Re=100 and 150.*

Re	Source	$\overline{\mathrm{Nu}}$	% deviation of $\overline{\mathrm{Nu}}$
100	Present work	5.589	-
	De and Dalal [5]	5.30	5.17
	Srikanth et al.[7]	5.562	0.48
150	Present work	7.161	-
	De and Dalal [5]	6.80	5.04
	Srikanth et al.[7]	7.127	0.48

When comparing the same with that of De and Dalal [5], the maximum deviations for Re=100 and Re=150 are less than 5.2%. The larger deviations in values of the average Nusselt numbers in the last case are due to the usage of a coarser grid by De and Dalal [5] in comparison to the grid used in the current study [7, 11]. All the results presented for validation are given at Ri=0 as no results are available for comparison at higher Richardson number for the range of parameters pertaining to the present set of conditions studied.

4.2 Flow patterns

The streamline patterns around an equilateral triangular bar (long in neutral direction) in a horizontal channel are presented in Fig. 3 for Ri=0, 1 and 2 at Re=1(a-c), Re=20(d-f) and Re=50(g-i) respectively. In order to analyze fluid flow characteristics, the flow patterns are presented and discussed for the steady regime with varying Richardson number. The figures clearly reveal that for Ri=0 (forced convection), the symmetry of the streamline contours is maintained about the mid plane for all the Reynolds numbers studied, however the symmetry of the streamlines is disturbed or lost as the value of Richardson number increases. The degree of asymmetry increases with increasing Richardson number because of buoyancy effect increases with Ri. As the magnitude of Ri increases, buoyancy is dominant and their exists insufficient kinetic energy to homogenize the fluid, leading to more velocity of fluid beneath the cylinder. Consequently, as the flow reaches towards the vertex of the triangular cylinder, most of the fluid rushes below the bottom face of the triangular cylinder. This causes an imbalance in the flow rate of the fluid above and below the cylinder leading to an asymmetrical flow. Moreover, no wakes form in the rear side of the triangular cylinder for Re=1, irrespective of Richardson number. However, with the increase in Reynolds number for $Ri \neq 0$, the wake region gradually increases but loses its symmetry because of the higher mass flow rate beneath the triangular bluff body. The similar observations are also reported by Dhiman et al. [16, 22] and Chatterjee and Amiroudine [25], but for the flow around square bluff body in the confined domain. The size of the vortices formed increases with the increasing Reynolds number till the flow is steady. However, on further increase in Reynolds number von Karman vortex street appears and flow becomes erratic and asymmetric.

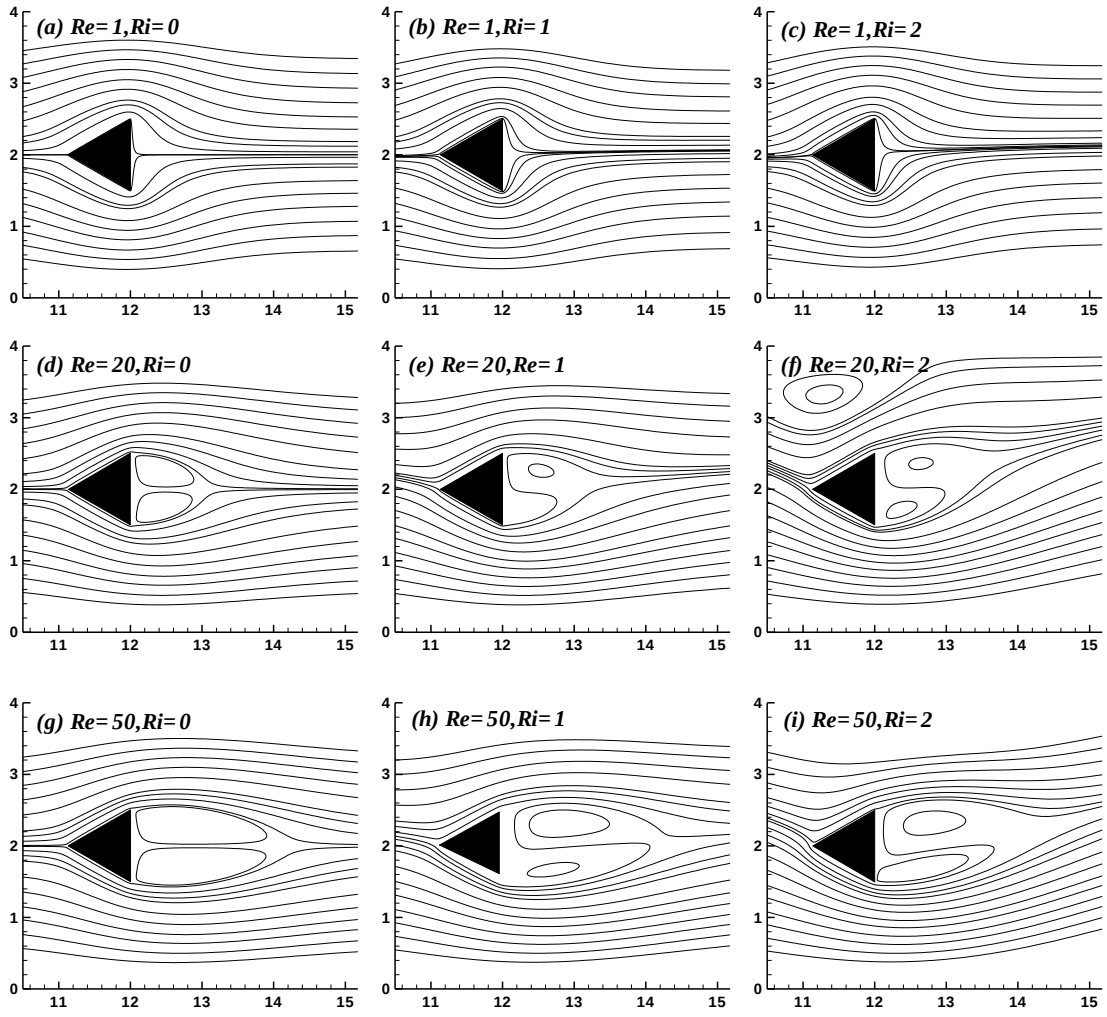

Figure 3: *Streamline contours for Ri=0,1 and 2 for Re=1 (a-c),Re=20 (d-f) and Re=50 (g-i) in steady regime.*

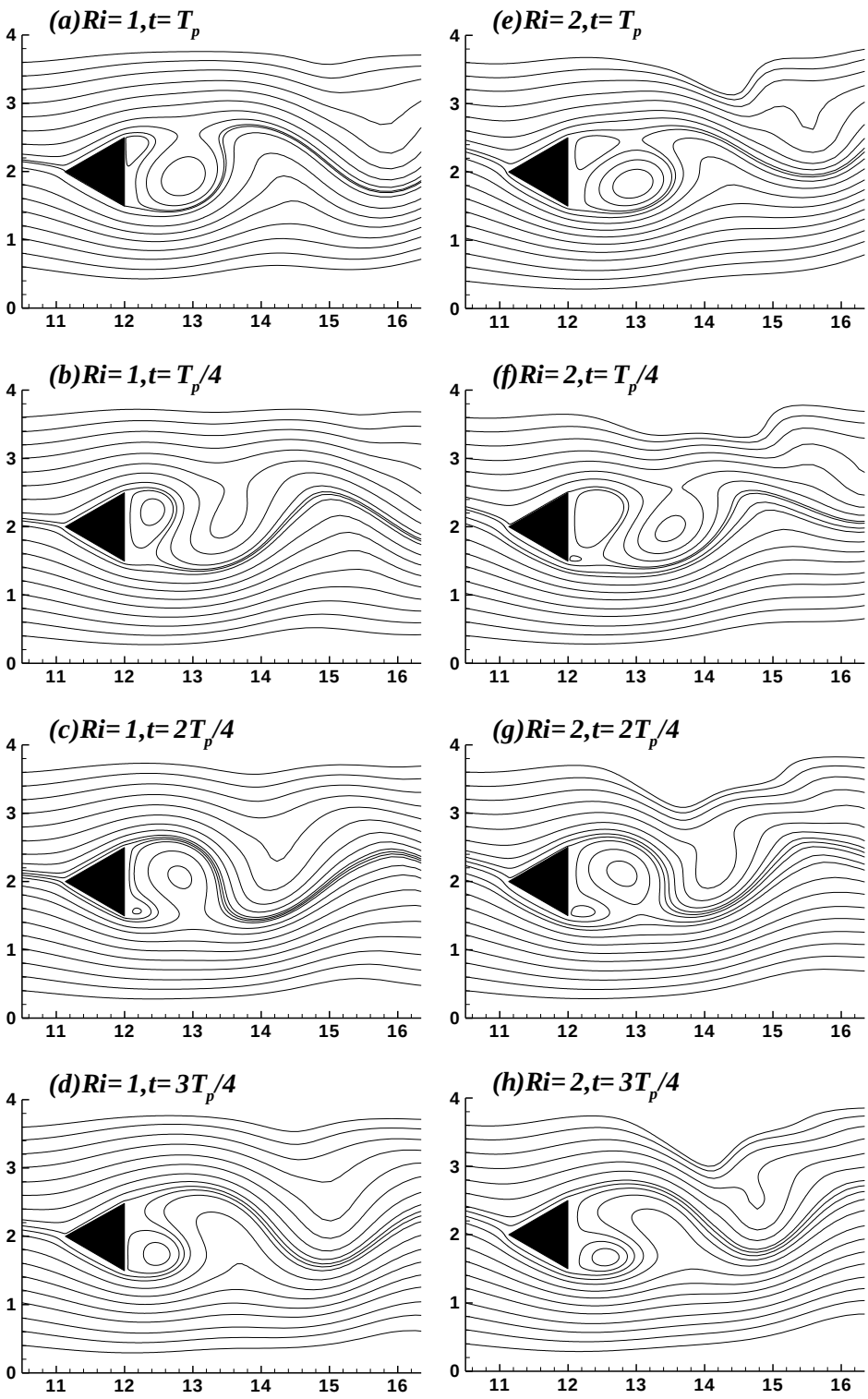

Figure 4: *Instantaneous streamlines for Re=100 for Ri=1 (a-d) and for Ri=2 (e-h) in time-periodic regime.*

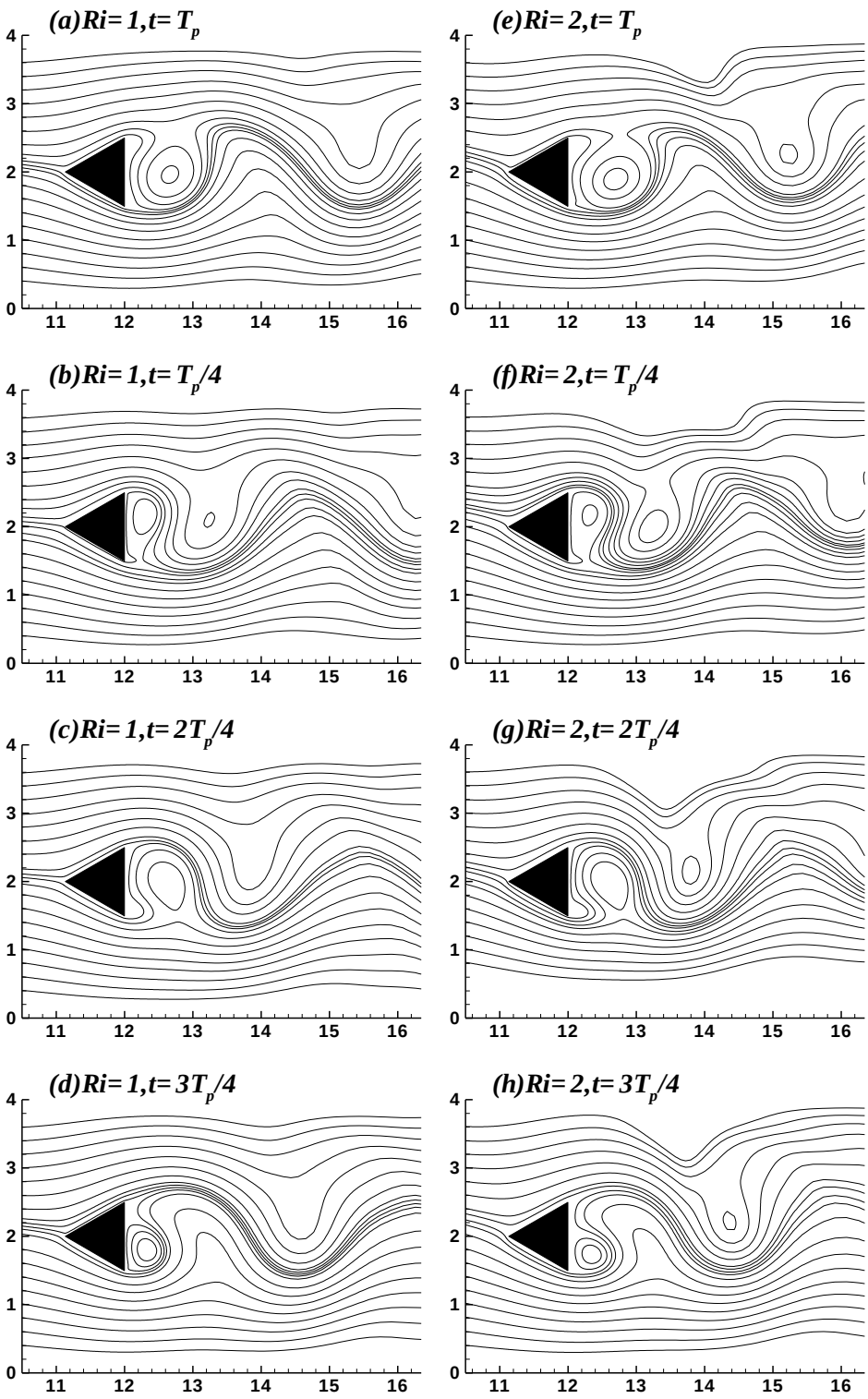

Figure 5: *Instantaneous streamlines for Re=150 for Ri=1 (a-d) and for Ri=2 (e-h) in time-periodic regime.*

For time-periodic regime, the instantaneous streamlines are given in Figs. 4 and 5 at Re=100 and 150 for Ri=1 and Ri=2 respectively. The instantaneous streamlines are shown for four successive moments of time viz. T_p, $T_p/4$, $2T_p/4$ and $3T_p/4$, thereby representing one whole time period for one cycle (T_p). It is observed that the frequency of vortex shedding increases with the increase in Richardson number, which is in agreement with the findings of Abbassi et al. [4] for the fluid flow around an isosceles triangular prism. The comparison of figures on the basis of Reynolds number at constant Richardson number clearly indicates that the frequency of vortex shedding is more behind the obstacle for higher Reynolds number. At the rear end corners of the triangular cylinder, the separation of flow occurs due to the fact that the present triangular cylinder is having a more or less a streamlined shape.

4.3 Wake length

The wake here is a disturbed fluid formed in the downstream region of a confined flow across the stationary bluff body. Fig. 3 presents the variation of the dimensionless recirculation length in addition to flow patterns. As is evident from Fig. 3, the wake or recirculation length increases monotonically with the increasing Reynolds number in the steady confined flow regime at Ri=0. Similar trend has been reported by Srikanth et al. [7] for an equilateral triangular cylinder and Dhiman et al. [26] in case of a square cylinder for a blockage ratio of 25% (confined flow). The separation of the flow and the wake formation take place at $Re \geq 5$ for all the ranges of Richardson numbers studied. However, as buoyancy comes into play (Ri>0), the wakes behind the long obstacle become asymmetric and the asymmetry increases with the increase in Reynolds number. Excellent studies on the control of flow separation and wake studies around bluff bodies of circular and square cross-section under the effect of thermal buoyancy can be found elsewhere [22, 27, 28].

4.4 Transition from a steady to an unsteady (time-periodic) regime

In the present study, the transitional parameters especially the Reynolds number are the group of parameters wherein the flow changes from steady behavior to (periodic) unsteady type. The Reynolds number at which this phenomena occurs is termed as critical Reynolds number (Re_c). Streamlines indicate that as Reynolds number gradually increases, flow separation takes place at the rear edge of the triangular cylinder giving rise to two symmetric standing vortices behind the obstacle on two sides of the middle axis at Ri=0.

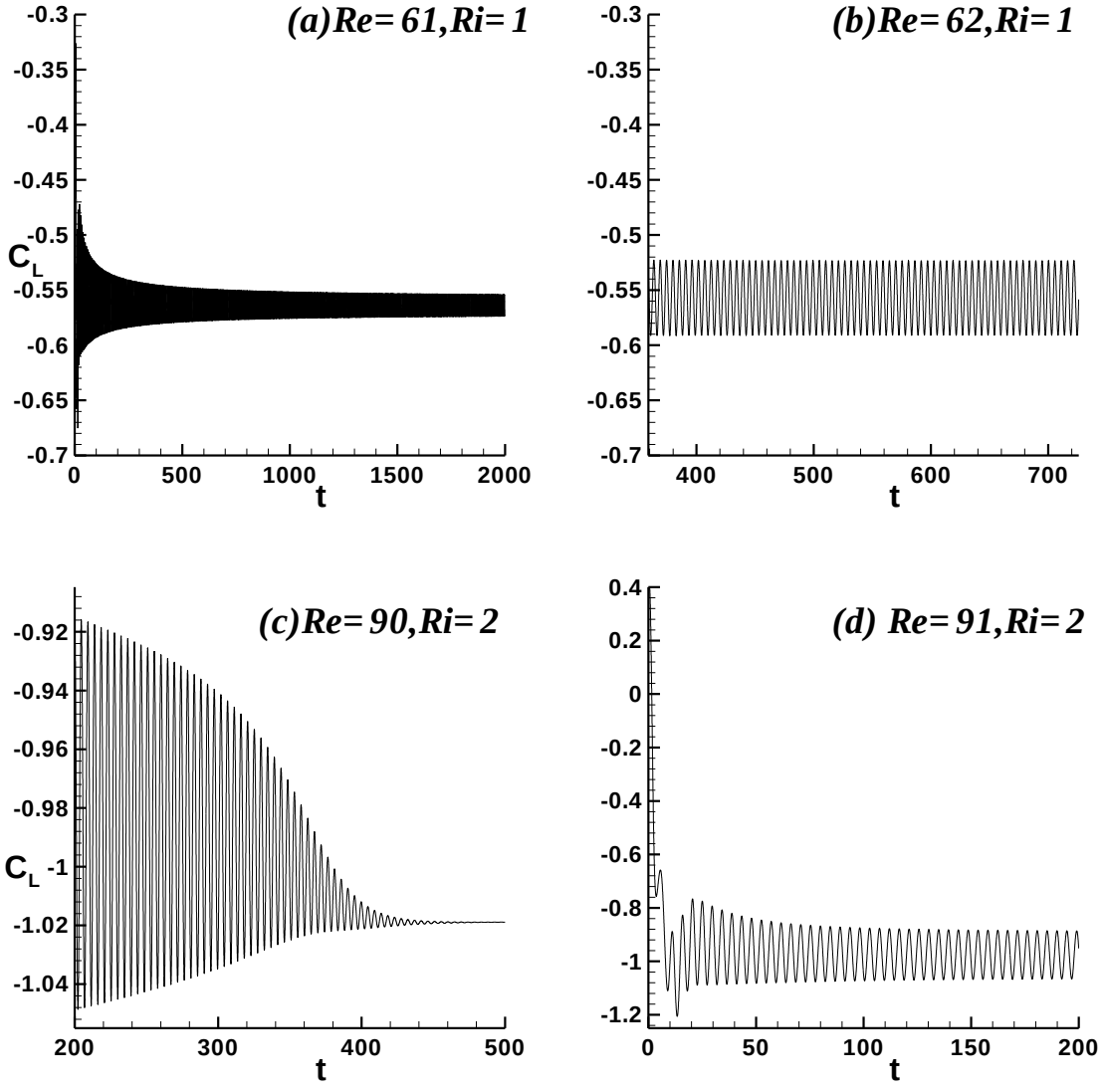

With

Figure 6: *Time history of a lift coefficient showing transition from a steady to unsteady time-periodic regime between (a-b) Re=61 and 62 at Ri=1 and (c-d) Re=90 and 91 at Ri=2.*

With the increasing Reynolds number the size of these vortices increases gradually (Fig. 3) and at some value of Re depending upon Ri the flow becomes time-periodic. This is the point of transition and the parameters are referred as critical parameters. To find out the values of critical Reynolds number for the ranges of this study, series of full domain computations were carried out while systematically increasing Reynolds number for each corresponding Richardson number. The study shows that Richardson number effects the critical Reynolds number to a greater extent beyond Ri=1. As reported by Abbassi et al. [4], the critical value of Reynolds number for the forced convection (Ri=0) across an isosceles triangular cylinder is 45. In an another study carried out by Srikanth et al. [7], the corresponding value comes out to be 58 for Ri=0, but for an equilateral triangular cylinder. The deviation is because in former case, a courser grid size of 105x21 has been taken as compared to the later one or the one used in this study with total number of 94,794 cells. Secondly, the discrepancy is because of the fact that Abbassi et al. [4] used an isosceles triangle with an aspect ratio of 0.5. The results of critical Reynolds number for Ri=0 are not replicated here as the same are reported in ref. [7], although verified by us. The results for transitional Reynolds numbers for Ri=1 and Ri=2 are presented in Fig. 6. Figures 6a-6b show the temporal history of the lift coefficients for the Reynolds numbers of 61 and 62 for Richardson number of 1, while as Figs. 6c-6d show the same for Reynolds numbers of 90 and 91 for Richardson number of 2, for an equilateral triangular cylinder of blockage ratio 25%. It is evident from the figures that how the transition of flow occurs from one Reynolds number to a succeeding Reynolds number in both the cases. It can be observed that the values of lift coefficients decay with time slowly and approach to steady state at Re=61 for Ri=1, while as the lift coefficient reaches steady state at Re=90 for Ri=2. In contrarily, the flow becomes unsteady or time-periodic in both the cases when Reynolds number increases to 62 (at Ri=1) and 91(at Ri=2). Thus the critical Reynolds number is found to increase with increasing buoyancy effects (or Ri).

4.5 Isotherm patterns

The thermal patterns close to the triangular cylinder are presented in Fig. 7 for different values of Richardson numbers for steady regime at Re=1(a-c), Re=20(d-f) and Re=50(g-i) respectively.

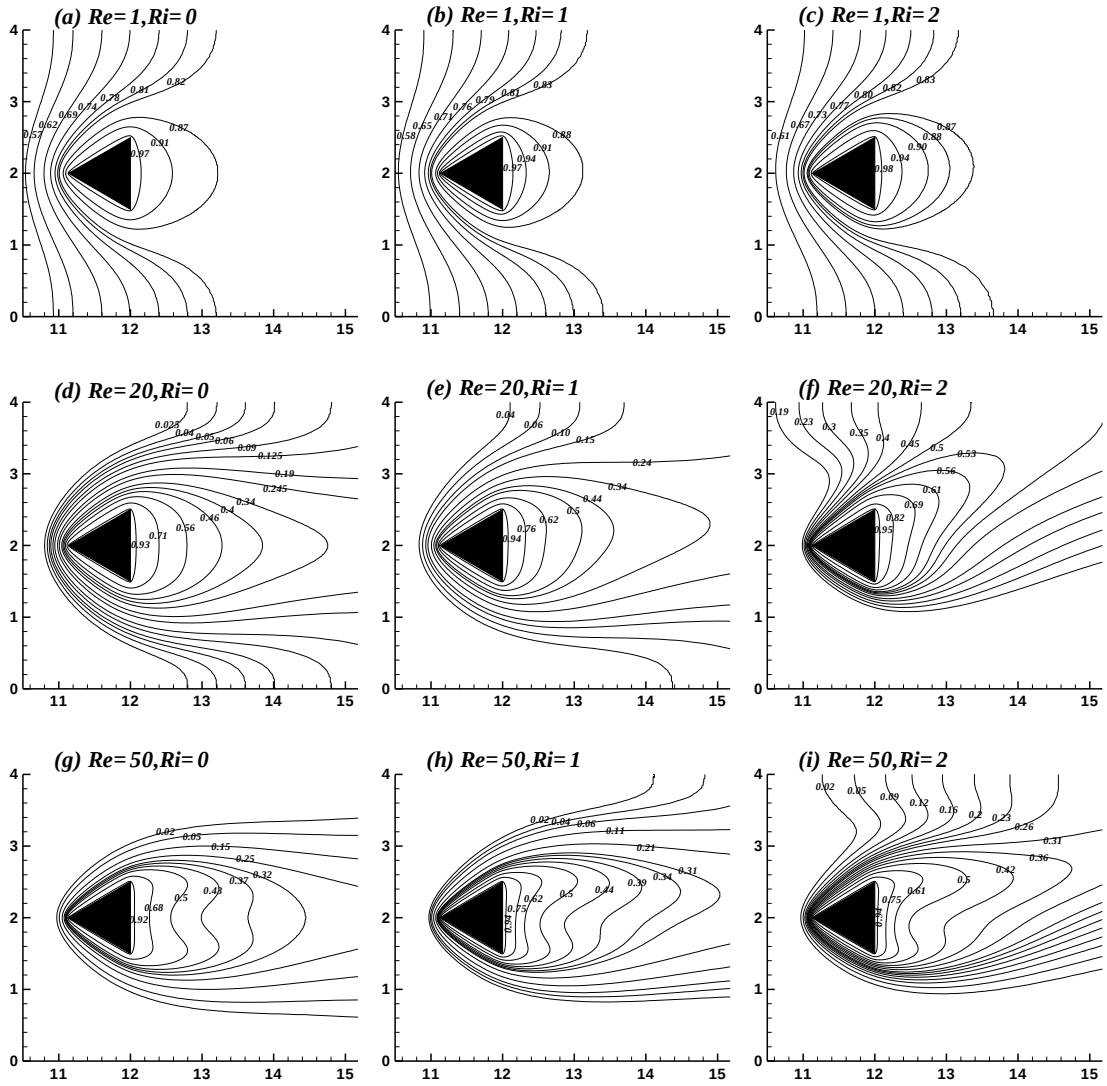

Figure 7: *Isotherm contours for Ri=0, 1 and 2 for Re=1 (a-c), Re=20 (d-f) and Re=50 (g-i) in steady regime.*

The Prandtl number is kept constant for all cases equal to 0.71.A close look on the isotherms shows that the buoyancy effects are observed negligible at Re=1 as the viscous forces are more dominant at low values of Reynolds number. However, the asymmetrical behaviour goes on increasing with the increase in Richardson number owing to the gradual increase in thermal buoyancy. This nature of isotherms also finds suitable resemblance with the isotherms presented by Dhiman et al. [16, 22] for the square cylinder under cross-buoyancy

For a time-periodic regime, the instantaneous isotherm patterns are given in Fig. 8 at Re=100 for Ri=1(a-d) and Ri=2(e-h). Another Fig. 9 shows the instantaneous isotherm patterns for Re=150 at Ri=1(a-d) and Ri=2(e-h). As observed, the increase in the Richardson number, increases the swirling vortices caused by unsteady separation of flow around the triangular cylinder. The effect is more prominent in the rear side of the bluff body. As the Reynolds number increase, asymmetry increases and the convective effects become stronger. Instantaneous isotherms show a wavering motion with stream wise stretching and bending which leads to separated patterns of fluid with different temperatures in the wake. The development of the thermal boundary layer that separates from the rear end vertices is effected by increasing Re to a larger extent. At Re=100, the localized heat transfer occurs near the rear end of the cylinder owing to crowding of isotherms. However, at Re=150, the figures reveal that isotherms no longer remain attached and bend sharply backwards thereby narrowing and thinning the recirculation region. Moreover, it is apparent from the figures that isotherms are crowded toward the front side of the triangular cylinder, resulting in higher heat transfer from the upstream side compared to any other side of the triangular cylinder.

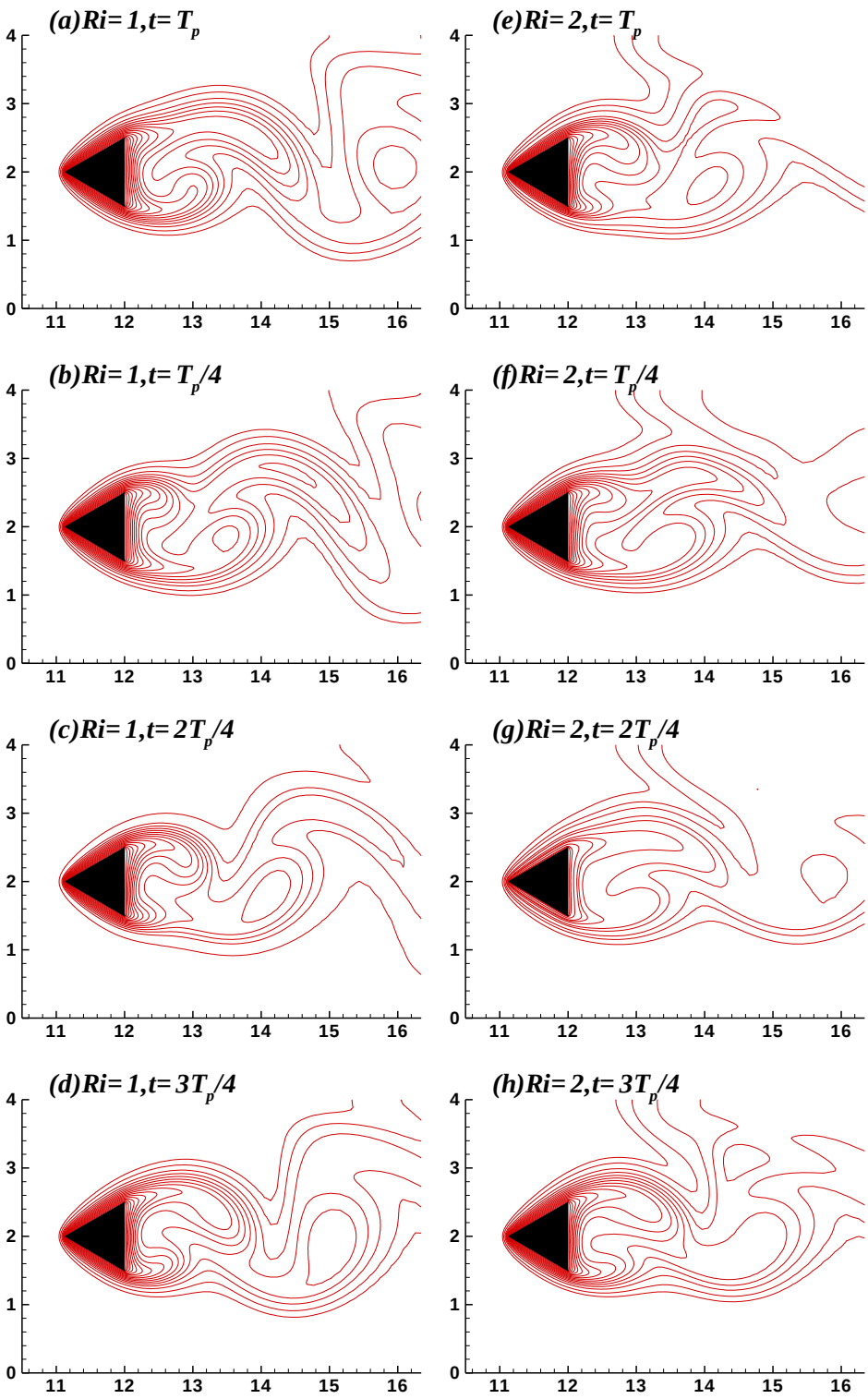

Figure 8: *Instantaneous isotherms for Re=100 for Ri=1 (a-d) and Ri=2 (e-h) in time-periodic regime.*

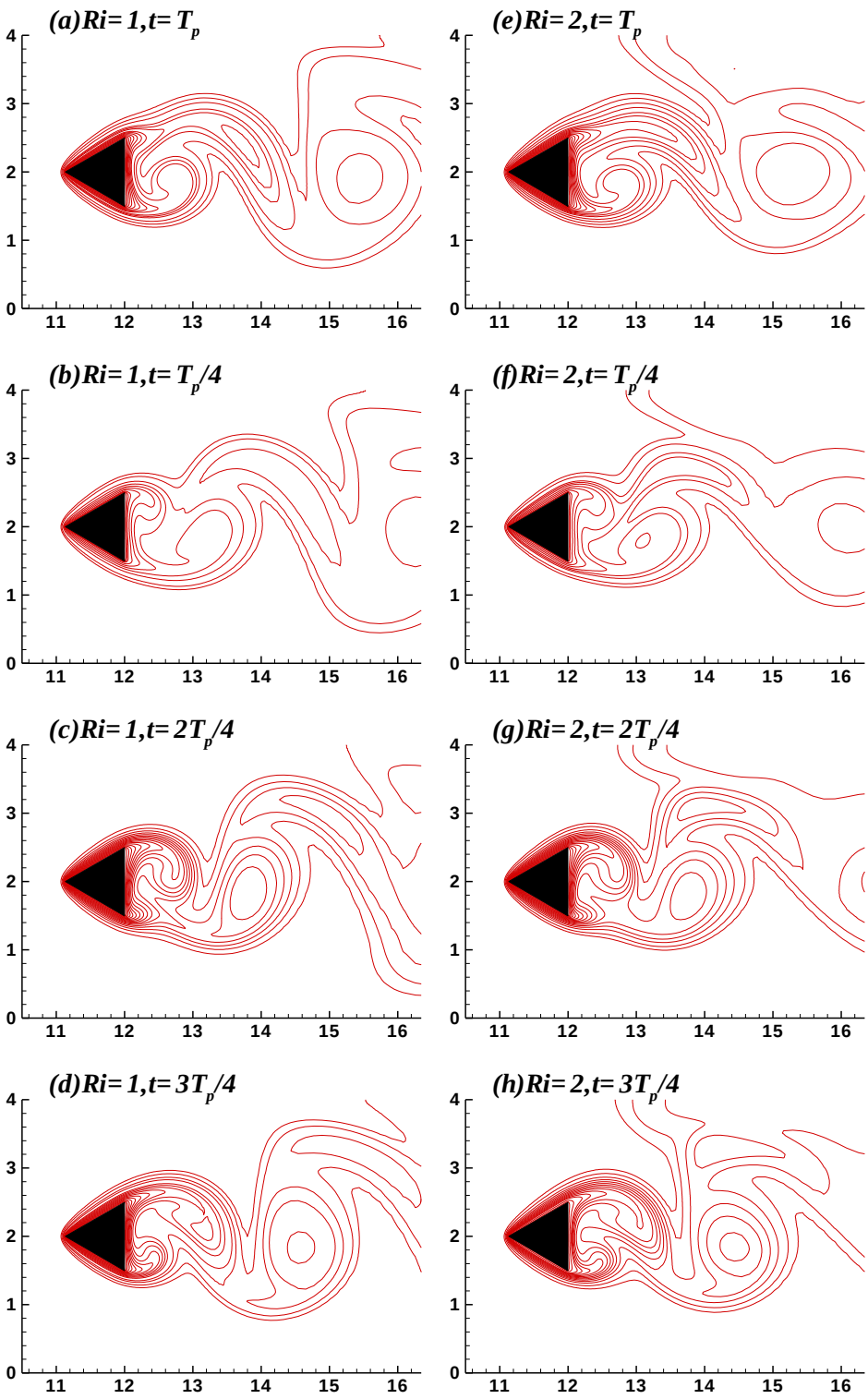

Figure 9: *Instantaneous isotherms for Re=150 for Ri=1 (a-d) and Ri=2 (e-h) in time-periodic regime.*

An additional simulations were carried out on the same system to find the effect of confinement on the fluid flow and heat transfer at varying Reynolds numbers from 20-40 for two different fluids with Prandtl numbers of 0.71 and 50. While observing the streamlines for Reynolds numbers 20 and 40 for two different working fluids with Prandtl number 0.71 and Prandtl number 50 respectively, there seems no significant variation or change of behaviour in streamlines for the Reynolds numbers studied, while changing the Prandtl number from 0.71 to 50. However, the flow is steady for the Reynolds numbers chosen in the present study at both the values of Prandtl numbers. The results reveal that the overall fluid flow pattern is almost insensitive to any change in the Prandtl number since the thermal field does not affect the flow field.

On the contrary, the isothermal patterns vary quite significantly with the Prandtl numbers. The fact is quite evident from the isothermal patterns shown in Fig. 10.

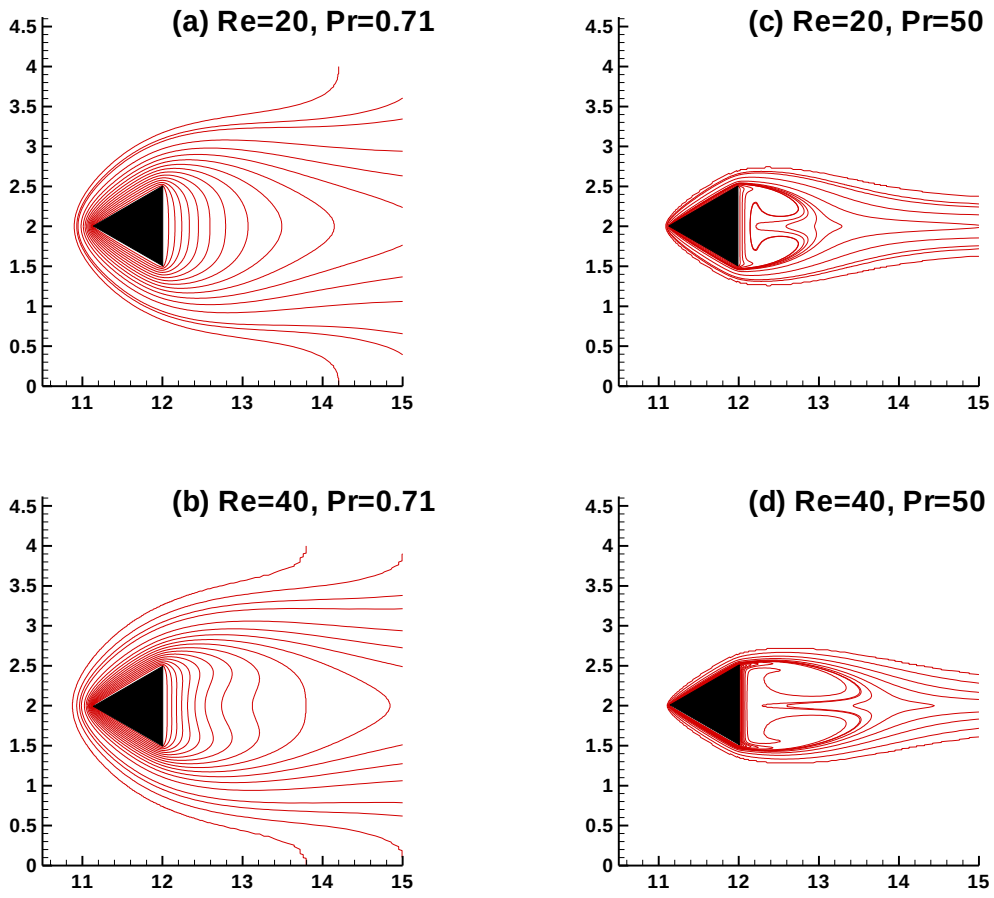

Figure 10: *Instantaneous isotherms at Re=20 and 40 for Prandtl number 0.71(a-b) and Prandtl number 50(c-d).*

The isotherms are presented for Reynolds numbers 20 and 40 for Prandtl number 0.71 and Prandtl number 50 in Figs. 10(a-b) and (c-d) respectively. As their exists wide variation in the thermal diffusivity on changing of Prandtl numbers, the same is depicted by the isotherms shown. The thermal diffusion is lower at lower Prandtl number (Pr=0.71), therefore the isotherms are wider around the triangular cylinder, but an opposite effect is observed on increasing the Prandtl number (Pr=50), wherein the isotherms get narrowed around the triangular cylinder because of the increasing effect of thermal diffusion. The results are in line with Chatterjee and Mondal [10].

4.6 Drag and lift coefficients

In fluid dynamics, the drag is referred as the sum of all forces acting on any solid bluff body in the direction of the flow velocity. As a result drag forces always decrease the fluid velocity by impeding the free flow of the fluid. This phenomena make the drag force highly dependent on the fluid velocity (Reynolds number). On the other hand, the lift coefficient is a dimensionless coefficient relating the lift generated by a bluff body to the density and the velocity of the fluid around the body and the associated area of the body. It is apparent that the components of the total drag coefficient (C_D) are frictional drag coefficient (C_{DF}) and pressure drag coefficient (C_{DP}). The variation of these parameters with increasing Reynolds number is shown in Figs. 11 and Fig. 13(a) at different Richardson numbers. Figures 11(a-b) give the variation of the two components of the overall drag coefficients and Fig. 11(c) shows the variation of their ratios with respect to Richardson numbers and Reynolds numbers in steady regime. As is evident from the figures at lower Reynolds numbers the drag coefficient is very high, but decreases fast in the range Re<10. Afterwards there seems very meager decrease in the drag coefficient with increasing Reynolds number. Thereafter, the total drag coefficient increases with further increase in Reynolds number (Re>100) for all the Richardson numbers, covered under this study (Fig. 11a). This behavior of drag coefficient and its components is because of the separation of flow with increasing Reynolds number, more prominent after Re>10. In other words, with an increase in Reynolds number, both viscous and pressure forces decrease especially due to the flow separation. Afterwards (Re>10), the pressure drag dominates the total drag with frictional drag hardly contributing to total C_D. The similar behavior is reported by De and Dalal [5] for

blockage ratio of 25% and Ri=0 for similar kind of system. The drag coefficient seems quite insensitive to the increasing value of Richardson number for the range presented in current study as the effect of Richardson number is more in the downstream side while the drag coefficient and its components are more sensitive to any changes in the upstream side of the bluff bodies. The soft response of the drag coefficient towards any change in Richardson number can be seen in Fig. 13(a). The response of drag towards increased Prandtl number of the working fluid is further illustrated in section 4.8.

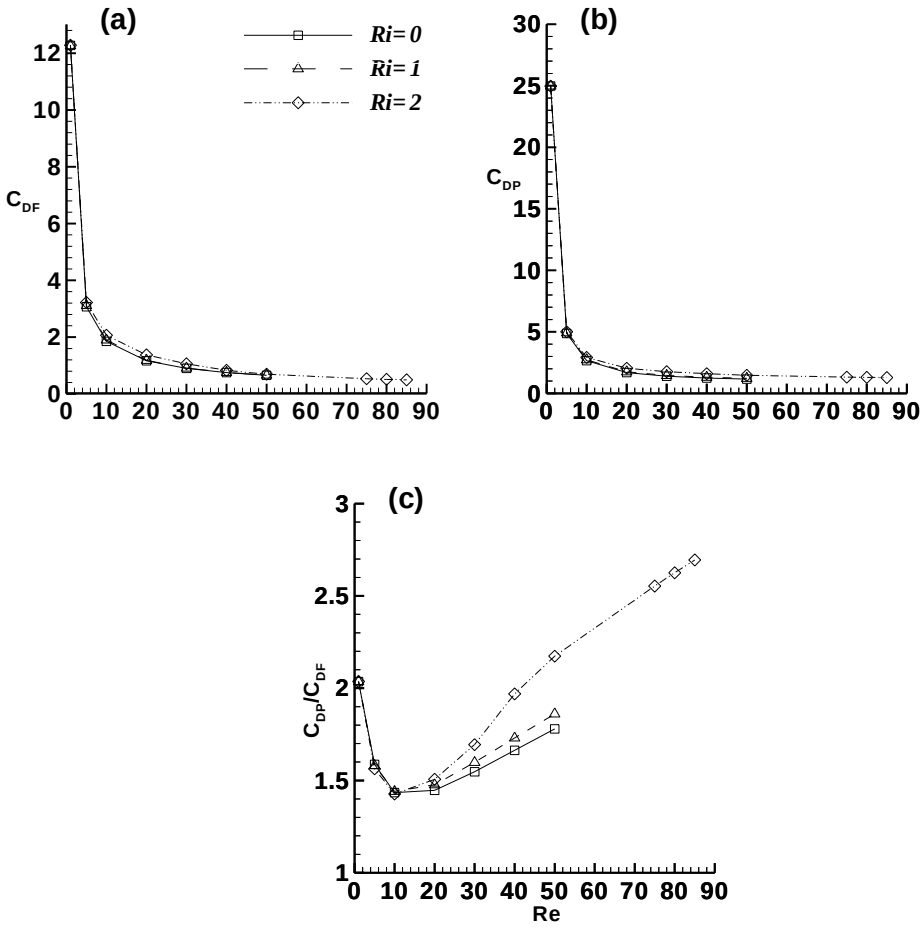

Figure 11: *Variation of (a) frictional drag coefficient (b) pressure drag coefficient and (c) ratio of pressure and fractional drag coefficients with Reynolds number at Ri=0, 1 and 2 in steady regime.*

The response of the lift coefficient to the changes in Reynolds number and Richardson number is presented in Fig. 13(b). In contrast to the drag coefficient, the lift coefficient is highly sensitive to the thermal buoyancy (Richardson number) as evident from the figure, especially at low values of Reynolds numbers. While changing the Richardson number from 0 to 1 and subsequently from 1 to 2, there is an average decrease of about 40% and about 32% respectively in the lift force for the ranges investigated. However, the behaviour of the lift coefficient at a constant Richardson number is quit similar to that of overall drag coefficient. Lift coefficient, a measure of wake oscillations, is first suppressed owing to the viscous effects till the Reynolds number reaches around Re=25 (Ri=1) and around Re=35 (Ri=2) and afterwards with increasing Reynolds number it shows an increasing trend in both the cases due to the strong convective effects. Furthermore, the buoyancy effects also come into play and increase the lift coefficient with increasing Richardson number. While switching over from forced convection (Ri=0) to cross-buoyancy mixed convection (Ri>0), more and more fluid rushes toward the lower surface of the 2-D triangular cylinder and flows beneath it, resulting in sufficient reduction in pressure at the top, leading to decrease in the lift coefficient at low Reynolds number but as soon as Reynolds number increases, the lift coefficient shows an increasing trend. The results are in line with Dhiman et al. [16,22] and Chatterjee and Amiroudine [25], for a square cylinder and the two side by side square cylinders respectively for the steady confined fluid flow regime under cross-buoyancy.

4.7 Vortex shedding and Strouhal number

The variation of Strouhal number (St) as a function of Richardson and Reynolds numbers is presented in Fig. 12. The results are presented for Richardson numbers 0, 1 and 2 in the periodic unsteady range, starting from their corresponding critical Reynolds numbers 59, 62 and 91 respectively. The results reveal that at a fixed Richardson number, there is a monotonical increases in Strouhal number (St) with the increase in Reynolds number. The behaviour is quite obvious as the vortices shed at a faster rate with increasing Reynolds number. The Strouhal number increases sharply up to Re=100 and afterwards the slope of St-Re curve shows a slight downfall for all cases of Ri studied. Due to the increased heating, the boundary layers along the surfaces of the long triangular bar get accelerated and subsequently bring an enhancement in the vortex shedding frequency (Strouhal number).The earlier forced convection studies by De and Dalal [5], Srikanth et al. [7] and Ali et al. [9] on a confined triangular bluff body have reported the similar trends. The observation i s also supported by the forced convection study of Durga Prasad and Dhiman [29] on a pair of square cylinders in a confined domain.

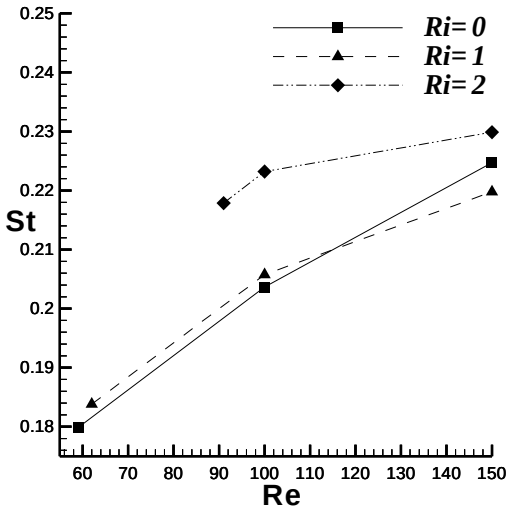

Figure 12: *Strouhal number (St) variation around the triangular cylinder with Reynolds number (Re) at Ri= 0, 1 and 2.*

4.8 Average Nusselt number

Figure. 13(c) describes the variation of the average Nusselt number ($\overline{\mathrm{Nu}}$) for an equilateral triangular cylinder under cross-buoyancy mixed convection along with its magnified view.

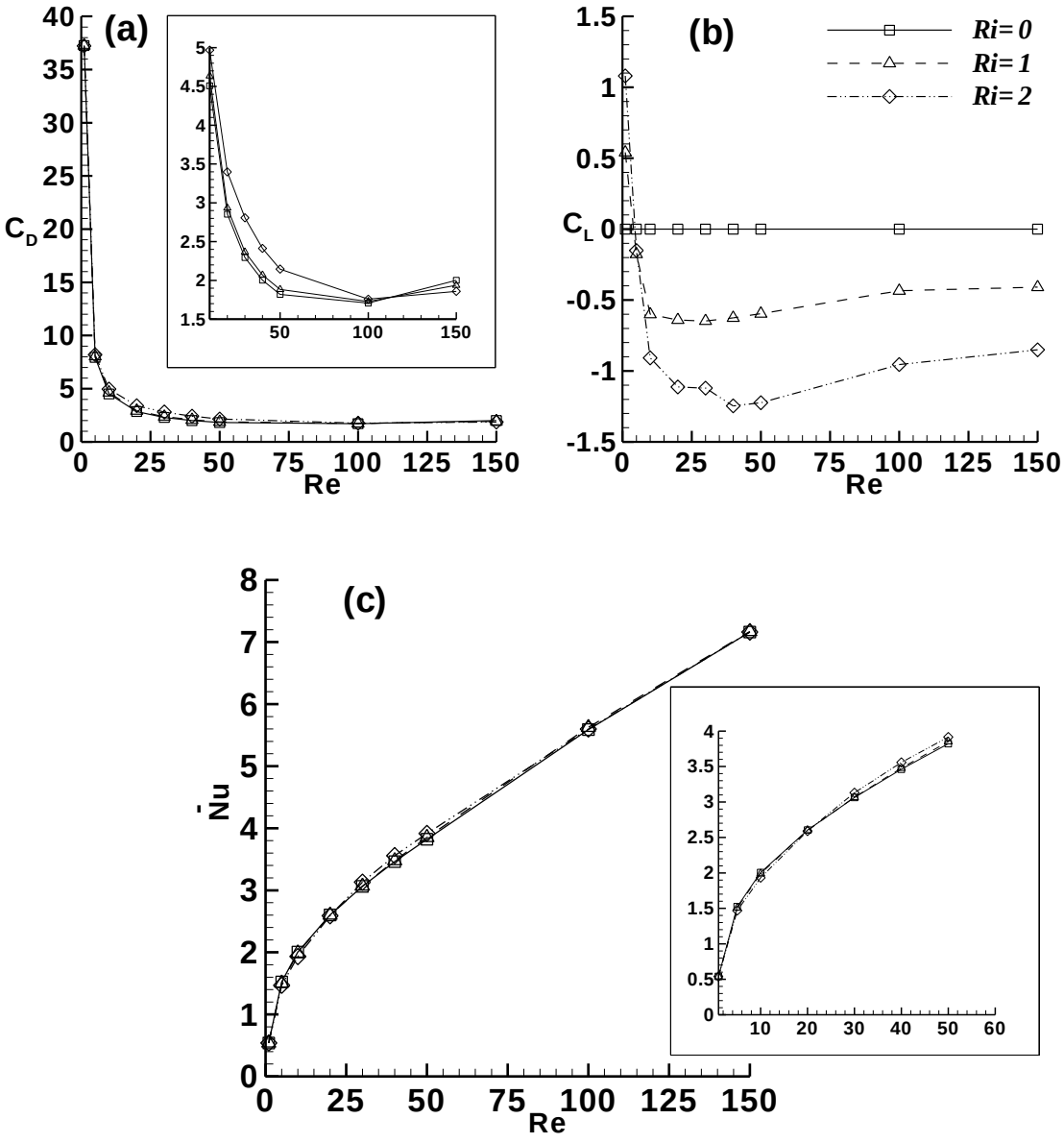

Figure 13: *Variation of (a) overall drag,(b) lift coefficients and (c) an average Nusselt number at different values of Reynolds number and Richardson number.*

An average Nusselt number representing the whole triangular cylinder is calculated by averaging the values of the local Nusselt number for surfaces of the whole cylinder for a steady fluid flow regime. However, in case of time-periodic unsteady flow, the surface average values are also time-averaged for at least ten number of cycles of vortex shedding. The average Nusselt number is found to increase with increasing Reynolds number owing to increased convection by the fluid particles which are responsible for higher rate of heat transfer. It is also observed that an average Nusselt number shows soft response towards any increase in the Richardson number at constant Reynolds numbers investigated. The potential energy of the fluid molecules is said to increase with the increase in Richardson number thereby increasing the diffusion transport rate of the fluid molecules, but not to such an extent to cause any noticeable change in the heat transfer. This observation is in agreement with some recent studies [16, 22] on the flow across a confined square cylinder under the impact of cross-buoyancy. The maximum percentage enhancement of approximately 4% is observed, for all the values covered under this study while comparing the corresponding values of the average cylinder Nusselt number at Ri=1 and 2 with respect to that at Ri=0.

Furthermore, to find out an intermediate values of the average Nusselt numbers, a simple heat transfer correlation (Eqn. 5) is given to establish a functional relationship among $\overline{Nu}$, Re and Ri. The correlation has been established from total number of six data points and is applicable for the Reynolds number range $20 \leq Re \leq 150$.

$$Nu = (0.57 + 0.001Ri)Re^{0.5} \qquad (5)$$

The given correlation has the average deviations of about 1.5% and 0.6% for Ri=0, 1 and 2, respectively while as the corresponding maximum deviations are observed to be about 5.4%, 4.8% and 3.3%, respectively.

As already stated in section 4.5, an additional simulations were carried out on the same domain to investigate the effect of changing working fluids (Pr=0.71 and 50) on heat transfer for the range of Reynolds numbers 20-40. The results reveal that there is no significant change in the overall drag coefficient (C_d) with respect to changing Prandtl number, owing to the fact that Prandtl number does not affect the overall flow pattern. The results are presented in Table-5 and further explained schematically in fig. 14.

Table 5: *Overall drag coefficient and percentage (%) enhancement in heat transfer for a triangular cylinder at Pr= 0.71 and 50 for various Reynolds numbers.*

Re	C_d		$\overline{Nu}$		Percentage(%) enhancement in $\overline{Nu}$
	Pr=0.71	Pr=50	Pr=0.71	Pr=50	
20	2.8544	2.8544	2.6032	11.3437	335.8
30	2.2950	2.2950	3.0632	13.9164	354.3
40	2.0037	2.0037	3.4617	16.0761	364.4

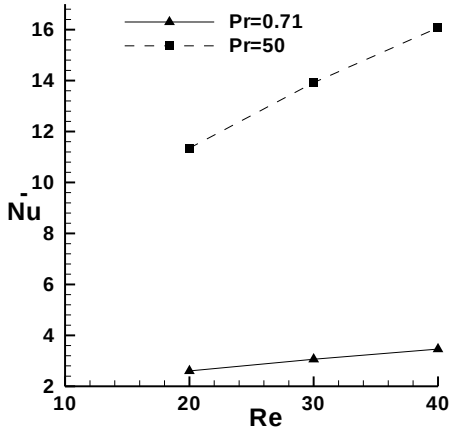

Figure 14: *Average Nusselt number variation with Reynolds number and Prandtl number.*

While demonstrating the effect of increasing Prandtl number on the average Nusselt number, the results elucidate that for a particular Reynolds number, the percentage enhancement is quite significant and the maximum percentage (%) enhancement in average Nusselt number is about 364.4% for Re=40. Percentage (%) enhancement in average Nusselt number is calculated as:

$$\left[\frac{\overline{Nu}_{Pr=50} - \overline{Nu}_{Pr=0.71}}{\overline{Nu}_{Pr=0.71}} x100\right]$$

The results show that an average Nusselt number increases monotonically with the increase in Reynolds number because of the increased convection currents. Figure 14 is presented to demonstrate as to how the Reynolds number and Prandtl numbers effect the heat transfer characteristics across a confined equilateral triangular cylinder. The results display fairly good agreement the available data in the literature [8].

CHAPTER 5

CONCLUSIONS AND RECOMMENDATIONS

In this study, the effects of cross-buoyancy mixed convection (Richardson number) have been numerically investigated for a confined equilateral triangular cylinder placed centrally at an axis of a horizontal channel with a blockage ratio of 25%. The investigation is done for the geometry where the vertex of a triangular cylinder is facing the fully developed parabolic flow of a Newtonian fluid (air) at constant Pr = 0.71. The range of investigation is taken as Re=1-150 and Ri= 0-2. The streamlines and isotherm contours for steady and periodic unsteady regimes are presented to describe the fluid flow and temperature profiles around the triangular cylinder. It is concluded that the drag coefficient shows a soft response towards Richardson number compared to that of lift coefficient, which shows an early decrease with increasing Reynolds numbers but later on shows an increasing trend due to the strong convective forces and buoyancy effects, for the conditions studied here. The calculations also reveal that the Richardson number effects the wake region on the rear side of the cylinder to a larger extent, which is one of the major factors in changing the values of global parameters in the downstream side. Similar to drag, an average Nusselt number shows a soft response to the changing Richardson number. The maximum percentage enhancement in an average Nusselt number is calculated to be around 3% for Re=40, for the values covered under this study while comparing the values of average Nusselt number at Ri=1 and 2 with respect to that at Ri=0. Finally, the critical Reynolds numbers for all the cases of changing Richardson numbers of 1 and 2 have been calculated. While the critical Reynolds number for the former case is Re=62, for later one it is found to be Re=91. The critical Reynolds number for Ri=0 is already been determined in ref. [7] as Re=59.

Recommendations for further work:

Following recommendations are made for future work in this field:

(a) The work can be extended for Non-Newtonian fluids particularly for calculating the transitional parameters.

(b) Though the present study is 2-D in nature, for more accurate results simulations in 3-D can be carried out for authentication as future work.

References

[1] Anderson, john D. (2004), Introduction to Flight, (5th edition) Section 4.20.

[2] Clancy L.J. Aerodynamics, Section 4.14.

[3] H. Abbassi, S. Turki, S.B. Nasrallah, Numerical investigation of forced convection in a plane channel with a built-in triangular prism, Int. J. Thermal Sci. 40 (2001) 649-658.

[4] H. Abbassi, S. Turki, S.B. Nasrallah, Mixed convection in a plane channel with a built-in triangular prism, Numer. Heat Transfer A 39 (2001) 307-320.

[5] A.K. De, A. Dalal, Numerical study of laminar forced convection fluid flow and heat transfer from a triangular cylinder placed in a channel, J. Heat Transfer 129 (2007) 646-656.

[6] M. Farhadi, K. Sedighi, A.M. Korayem, Effect of wall proximity on forced convection in plane channel with a built-in triangular cylinder, Int. J. Thermal Sci. 49 (2010) 1010-1018.

[7] S. Srikanth, A.K. Dhiman, S. Bijjam, Confined flow and heat transfer across a triangular cylinder in a channel, Int. J. Thermal Sci. 49 (2010) 2191-2200.

[8] H. Chattopadhyay, Augmentation of heat transfer in channel using a triangular prism, Int. J. Thermal Sci. 46 (2007) 501-505.

[9] M. Ali, O. Zeitoun, A. Nuhait, Convective heat transfer around a triangular cylinder in an air cross flow, Int. J. Thermal Sci. 50 (2011) 1685-1697.

[10] D. Chatterjee, B. Mondal, Forced convection heat transfer from an equilateral triangular cylinder at low Reynolds numbers, Heat Mass Transfer 48 (2012) 1575-1587.

[11] A.K. Dhiman, S. Kumar, Non-Newtonian power-law flow across a confined triangular bluff body in a channel, Korean J. Chem. Eng. 30 (2013) 33-44.

[12] S. El-Sherbiny, Flow separation and reattachment over the sides of a 90^0 triangular prism, J. Wind Eng. Ind. Aerodyn. 11 (1983) 393-403.

[13] A.L. Csiba, R.J. Martinuzzi, Investigation of bluff body asymmetry on the properties of vortex shedding, J. Wind Engg. Ind. Aerodyn. 96 (2008) 1152-1163.

[14] G.V. Longo, G. Buresti, Experimental investigation on the aerodynamic loads and wake flow features of low aspect-ratio triangular prisms at different wind directions, J. Fluids Structures 25 (2009) 1119-1135.

[15] M.A. Hassab, M.A. Teamah, W.M El-Maghlany, M.A. Kandil, Experimental study for a mixed convection heat transfer from an isothermal horizontal triangular cylinder, Int. J. Eng. Sci. 22 (2013) 210-225.

[16] A.K. Dhiman, R.P. Chhabra, V. Eswaran, Steady mixed convection across a confined square cylinder, Int. Comm. Heat Mass Transfer 35 (2008) 47-55.

[17] D. Chatterjee, B. Mondal, Effect of thermal buoyancy on vortex shedding behind square cylinder in cross flow at low Reynolds numbers, Int. J. Heat Mass Transfer 54 (2011) 5262-5274.

[18] A.K. Dhiman, R. Ghosh, Computer simulation of momentum and heat transfer across an expanded trapezoidal bluff body, Int. J. Heat Mass Transfer 59 (2013) 338-352.

[19] Bird, R.B., Stewart, W.E., Lightfoot, E.N., Transport Phenomena, 2nd edition, Wiley, New York.

[20] ANSYS, Inc., 2009, ANSYS FLUENT 12.0 User's Guide, U.S.A.

[21] A.K. Dhiman, N. Anjaiah, R.P. Chhabra, V. Eswaran, Mixed convection from a heated square cylinder to Newtonian and power-law fluids, J. Fluids Eng. 129 (2007) 506-513.

[22] A.K. Dhiman, N. Sharma, S. Kumar, Wall effects on the cross-buoyancy around a square cylinder in the steady regime, Brazilian J. Chem. Eng. 29 (2012) 253-264.

[23] J. Robichax, S. Balachandar, S.P. Vanka. Two-dimensional floquet instability of the wake of square cylinder, Phys. Fluids 11 (1999) 560-578.

[24] S.C. Luo, X.H. Tong, B.C. Khoo, Transition phenomena in the wake of a square cylinder, J. Fluids Struc. 23 (2007) 227-248.

[25] D. Chatterjee, S. Amiroudine, Two-dimensional mixed convection heat transfer from confined tandem square cylinders in cross-flow at low Reynolds numbers, Int. Comm. Heat Mass Transfer 37 (2010) 7-16.

[26] A.K. Dhiman, R.P. Chabra, V. Eswaran, Flow and heat transfer across a confined square cylinder in the steady flow regime: effect of Peclet number, Int. J. Heat Mass Transfer 48 (2005) 4598-4614.

[27] Dhiman, N. Sharma, S. Kumar, Buoyancy aided momentum and heat transfer in a vertical channel with a built-in square cylinder, Int. J. Sustainable Energy, 2013, DOI: 10.1080/14786451.2013.764878.

[28] D. Chatterjee, B. Mondal, Control of flow separation around bluff obstacles by superimposed thermal buoyancy, Int. J. Heat Mass Transfer 72(2014) 128-138.

[29] A.V.V.S. Durga Prasad, A.K. Dhiman, CFD analysis of momentum and heat transfer around a pair of square cylinders in side -by-side arrangement, Heat Transfer Eng. 35(2014) 398-411.